NASA TECHNICAL NOTE

NASA TN D-2518

NASA TN D-2518

EFFECTS OF DIELECTRIC COVERS OVER SHUNT SLOTS IN A WAVEGUIDE

by William F. Croswell and Robert B. Higgins

Langley Research Center

Langley Station, Hampton, Va.

NATIONAL AERONAUTICS AND SPACE ADMINISTRATION • WASHINGTON, D. C. • DECEMBER 1964

EFFECTS OF DIELECTRIC COVERS OVER SHUNT SLOTS IN A WAVEGUIDE

By William F. Croswell and
Robert B. Higgins

Langley Research Center
Langley Station, Hampton, Va.

NATIONAL AERONAUTICS AND SPACE ADMINISTRATION

For sale by the Office of Technical Services, Department of Commerce,
Washington, D.C. 20230 -- Price $1.25

EFFECTS OF DIELECTRIC COVERS OVER SHUNT SLOTS IN A WAVEGUIDE

By William F. Croswell and
Robert B. Higgins
Langley Research Center

SUMMARY

The purpose of this study was to determine experimentally the effects of placing a dielectric cover over a shunt slot in a waveguide. Slot lengths and displacements were chosen so that the data cover the waveguide bandwidth for dielectric constants from 1 to 4. Formulas are developed, by utilizing the measured data, for the mean values of slot conductance and resonant frequency where the cover thickness is greater than one-fourth of the wavelength in the dielectric material at resonance. In addition, it is shown that plane wave theory gives a bound on the conductance variation for covers thicker than one-fourth of the wavelength in the dielectric material. Pattern and voltage-standing-wave-ratio (VSWR) measurements of linear arrays of dielectric-covered slots designed from single-slot data are presented along with predicted patterns and VSWR for comparison.

INTRODUCTION

A space vehicle reentering the earth's atmosphere at hypersonic velocities will be subject to severe environmental conditions in the form of extreme structural loads, heat-transfer rates, and temperatures. In order to protect the internal instrumentation systems of such vehicles from excessive heat, common use is made of dielectric ablative materials which cover the external structural surfaces including the antennas. Trajectories of space-vehicle flight frequently contain long time periods before and after reentry. Antennas used for such applications must operate satisfactorily throughout the trajectory exclusive of reentry plasma effects, a separate problem. Since the ablation process results in a change in material thickness, antennas proposed for such an application must be relatively insensitive to these changes in addition to fulfilling the usual minimum-weight and volume requirements. An antenna which meets many of these requirements at microwave frequencies is the shunt slot in a waveguide. However, use of a slot array in this application requires an extensive knowledge of slot characteristics as a function of the thickness and dielectric constant of the covering material.

Past interest in dielectric-covered shunt-slot waveguide arrays has been generally restricted to the problem of providing a fixed thin radome or

pressurizing seal for conventional radar-antenna application. In those instances, it has been noted that severe changes occurred in the array characteristics when a thin cover was placed over slots that were designed from free-space data (p. 32-5 of ref. 1). In other instances, data have been obtained which include cover effects for a particular array design (ref. 2) but which are restricted to fixed thin covers of a particular dielectric material.

Ablation materials, however, cannot be restricted to thin fixed layers because of heat-protection requirements and the loss of material during reentry. Therefore, data which encompass a wide range of material thicknesses and dielectric constants are required for reentry antenna design. An exact theoretical solution to this problem appeared to be exceedingly difficult since any solution will require a detailed knowledge of the local reactive slot fields with and without the presence of a dielectric. Therefore, the experimental approach was used and approximate theories were developed from analysis of measured results. Part of the data obtained in this study has been presented in reference 3.

SYMBOLS

a	broad dimension of waveguide
b	narrow dimension of waveguide
c	arbitrary constant
d	radial distance
d'	spacing between elements
d_1	distance in medium 1
d_2	distance in medium 2
$E(\theta)$	normalized electric-field intensity at angle θ
$E_1(\theta)$	element pattern of idealized slot
f	frequency
f_o	free-space slot resonant frequency
f_R	average resonant frequency
g_n	normalized conductance

$$g_1 = 2.09 \frac{\lambda_g}{\lambda_o} \frac{a}{b} \cos^2 \frac{\pi \lambda_o}{2\lambda_g}$$

I	current
l	length of slot
n	number of sources
P_r	coupled power
P_d	coupled power into dielectric
P_o	coupled power into free space
R_r	radiation resistance
r	voltage reflection coefficient for single interface
t	thickness of dielectric cover
V_o	slot excitation voltage
W	net radial propagating reactive energy
x	slot displacement, measured from waveguide center line to slot center line
$\beta = \frac{2\pi}{\lambda_o}$	
ϵ	relative dielectric constant
ϵ_{equiv}	equivalent relative dielectric constant
ϵ_o	permittivity of free space
ϵ_1	relative dielectric constant of medium 1
ϵ_2	relative dielectric constant of medium 2
η	intrinsic impedance
θ	angle between normal to array plane and far-field observation point
λ_g	waveguide wavelength
λ_o	free-space wavelength
λ_ϵ	wavelength in dielectric at average resonant frequency

μ_o permeability of free space

ρ voltage reflection coefficient

EXPERIMENT

For this experiment, the slots were fabricated by a process in which electrode burning is used as a means of removing the metal. The size and shape of the slot are determined by the size and shape of the electrode. This method provides a means of fabricating very long arrays and sustaining required dimensional precision. Rectangular-shaped slots of standard width, 0.062 inch, formed in an RG 52/U waveguide constitute the samples used in this experiment.

In order to cover the waveguide bandwidth, it was found necessary to use at least eight samples as shown in table I.

Figure 1 shows the arrangement of a typical sample under test. The waveguide section containing the slot is approximately 8 inches long. The variable short was required for making measurements over the waveguide bandwidth. It was determined experimentally that the 6-inch ground plane is of sufficient size to simulate infinite ground-plane conditions as far as slot-conductance measurements are concerned.

Standard waveguide measurement methods were employed for determining normalized conductance values. The insertion technique, using precision calibrated attenuators, was used for measurement of high voltage standing-wave ratio (VSWR) as given in reference 4. Because of the relatively low values of conductance being measured, extra care was required in regard to line discontinuities at the junctions. Also, the readings had to be corrected for waveguide wall losses.

The four dielectric materials listed in table II were investigated. Measurements were taken at several discrete thicknesses. An attempt was made to cover the dielectric-constant range which includes many of the natural dielectrics.

EXPERIMENTAL RESULTS

Free Space

The experimental results for the slots with no dielectric cover are presented in figure 2 in the form of normalized resonant conductance plotted as a function of resonant frequency for various displacements x. Equations relating physical dimensions to resonant conductance have been developed (ref. 5) and are presented as equations (7) and (8) of this report. The curves in figure 2 were calculated on the basis of these equations and the pertinent dimensions. The validity of the equations has been demonstrated by experimental values taken on round-end slots (see pp. 9-3 - 9-5 of ref. 5). The coincidence of curves and

measured points in this figure would appear to extend the validity to include rectangular-shaped slots as well.

Measured values of resonant length are given in figure 3 with l/λ_o plotted as a function of λ_o/λ_g for various displacements x. Note the apparent dependence of the resonant-length ratio on λ_o/λ_g as well as on x.

Dielectric Cover

The experimental results for dielectric-covered slots are given in figures 4 to 11 where the dielectric constant ϵ is the major differentiating parameter. Each plot contains a series of curves where the normalized slot conductance is plotted against frequency for various dielectric-cover thicknesses. Table II is given as an index to the data.

ANALYSIS OF DATA

General

A study of the measured data reveals the fact that gross changes in the slot characteristics occur with the addition of a dielectric cover. However, the slots do maintain a resonant behavior. The changes in slot characteristics can be summarized in the following three observations:

1. The frequency at which resonance occurs (defined as the frequency at peak conductance) decreases radically as a function of cover thickness up to a thickness of $0.20\lambda_\epsilon$. For cover thicknesses greater than $0.20\lambda_\epsilon$, the resonant frequency varies sinusoidally with a period of $0.5\lambda_\epsilon$. (See figs. 4, 5, 6, and 7.)

2. A significant reduction of normalized conductance g_n occurs with the addition of a dielectric cover for thicknesses up to approximately $0.20\lambda_\epsilon$. For thicknesses greater than $0.20\lambda_\epsilon$, the peak conductance varies sinusoidally, with a period of approximately $0.5\lambda_\epsilon$. (See figs. 9, 10, and 11.)

3. The resonant conductance is much lower than that predicted for the slot with no dielectric cover. (See fig. 2 and table III.)

Analyses presented in succeeding paragraphs give first-order predictions for all three of the major effects listed previously. In order to make these analyses, it was necessary to define an average resonant frequency f_R which is a function of the dielectric constant ϵ, is not a function of the slot displacement x or dielectric-cover thickness t, and is dependent on slot length l. To accomplish this, for a particular dielectric constant, plots of resonant frequency as a function of thickness were made from the measured data for each of eight samples. By inspecting these curves in the region where the resonant frequency was

periodic as a function of thickness, the average frequency for each sample was determined. Then, by using the slot length l and the average frequency, a value of l/λ_o was calculated for each sample. All eight values of l/λ_o were averaged to obtain a value related to the particular dielectric constant. This last averaging process was necessary to eliminate the secondary effects of waveguide wavelength from the data. By utilizing this process the plot shown in figure 8 was obtained. With a knowledge of the dielectric constant ϵ and the slot length l, an average resonant frequency pertaining to ϵ is defined. The vertical dashed lines given in the measured data in figures 4 to 7 indicate the appropriate defined average resonant frequency f_R.

Slot Conductance as a Function of Cover Thickness

Of major interest is the variation of the slot conductance as a function of cover thickness. By use of the definition of average resonant frequency, values were obtained from the measured data and are presented as slot conductance plotted against the cover thickness expressed in wavelengths t/λ_ϵ. Figures 9 to 11 are such plots for slot displacements $x = 0.066$ inch, 0.093 inch, and 0.136 inch, where $l = 0.475$ inch and all dielectrics are considered. From inspection of these and similar curves, it was noted that these curves became periodic with λ_ϵ after a cover having a thickness of $0.20\lambda_\epsilon$ was added. This fact suggested the application of plane wave theory to this problem. From pages 32-4 to 32-23 of reference 1, and with normal incidence and lossless dielectrics assumed, the voltage reflection coefficient for a plane dielectric sheet with a plane wave incident is given by

$$\rho = \frac{r\left(1 - e^{-\frac{j4\pi t\sqrt{\epsilon}}{\lambda_o}}\right)}{1 - r^2 e^{-\frac{j4\pi t\sqrt{\epsilon}}{\lambda_o}}} \tag{1}$$

where

$$r = \frac{1 - \sqrt{\epsilon}}{1 + \sqrt{\epsilon}}$$

when the extreme cases of thickness are considered, ρ may be expressed

$$\left|\rho\right|_{t = \frac{n}{2}\lambda_\epsilon} = 0 \tag{2}$$

and

$$\left|\rho\right|_{t=\frac{(2n+1)}{4}\lambda_\epsilon} = \left|\frac{2r}{1+r^2}\right| \tag{3}$$

where $n = 1, 2, 3 \ldots$. To relate this information to the curves in figures 9 to 11, it is assumed that the place where the maximum value of conductance occurs corresponds to the case of no reflections as given by equation (2). The first case corresponding to equation (2) occurs at $t \approx 0.65\lambda_\epsilon$ for all dielectric constants. It is assumed that maximum power is coupled out of the slot at this thickness. In order to compute the effect of maximum reflection as predicted by equation (3), the amount of power coupled out of the slot at $t \approx 0.65\lambda_\epsilon$ is reduced by $\left|\rho\right|^2_{t=\frac{(2n+1)}{4}\lambda_\epsilon} = \left(\left|\frac{2r}{1+r^2}\right|\right)^2$ and converted into conductance. The dashed lines shown in figures 9 to 11 are the bounds on the conductance as a function of dielectric thickness, with the upper line corresponding to no reflections and the lower one to maximum reflections. For a cover thickness greater than $0.20\lambda_\epsilon$ these bounds appear to give a useful prediction for conductance variations.

Change in Slot Conductance From Free-Space Values

From the preceding analysis and an inspection of the measured data, it is obvious that plane-wave—plane-sheet theory alone is not satisfactory for predicting the change in slot conductance that occurs with a change from the uncovered slot to the covered slot. The purpose of this discussion is to obtain a primary prediction of slot conductance that is strictly a function of the dielectric constant.

From reference 6 the radiation resistance of a resonant half-wave slot in an infinite ground plane may be written

$$R_r = \frac{1}{4 \times 73}\eta^2 \tag{4}$$

where η is intrinsic impedance.

For the case of the slot located in a waveguide, the radiation resistance R_r is double the value given by equation (4) since the slot can radiate only in one direction (p. 295 of ref. 7). Placing a dielectric cover over the slot does not appear to produce any significant changes in the internal fields of the

waveguide and the internal wall currents which excite the slot, if the cover is of the proper thickness $\left(t \approx 0.65\lambda_\epsilon + \frac{n\lambda_\epsilon}{2}\right)$ so that reflections are small. By restricting interest to the case of no reflections and assuming the waveguide and slot to be equivalent to a constant current source I operating into the radiation resistance R_r, the power coupled out of the slot is given by

$$P_r = \frac{I^2}{2 \times 73} \frac{\mu_o}{\epsilon_o \epsilon} \tag{5}$$

In equation (5) the entire half space outside the waveguide is considered to be completely filled with the material having a dielectric constant ϵ. If P_o is the power coupled out of the slot resonant with an external medium μ_o, ϵ_o and P_d is the power coupled out of the slot resonant with an external medium μ_o, ϵ, then from equation (5)

$$P_d = \frac{P_o}{\epsilon} \tag{6}$$

From reference 5 the normalized conductance of a resonant shunt slot with no cover is given by

$$g_n = g_1 \sin^2 \frac{\pi x}{a} \tag{7}$$

where

$$g_1 = 2.09 \frac{\lambda_g}{\lambda_o} \frac{a}{b} \cos^2 \frac{\pi \lambda_o}{2\lambda_g} \tag{8}$$

A calculated value of conductance for shunt slots with a dielectric cover can be obtained by using these equations and the result given by equation (6). However, it must be remembered that a slot of given length will resonate at a lower frequency with the addition of a cover and that, from equation (7), the slot conductance is a function of λ_g/λ_o. Therefore, either the average resonant frequency must be used to calculate λ_o or, if a particular operating frequency is desired, the physical length l must be adjusted according to figure 8. To obtain calculated values the following procedure is used:

1. For a given slot displacement x, the slot conductance is calculated from equations (7) and (8). The average resonant frequency is used for a particular ϵ to determine the resonant frequency.

2. This value of conductance is converted to radiated power and reduced by $1/\epsilon$ as indicated in equation (6).

3. The reduced value of power is converted back to normalized slot conductance g_n.

Table III shows the comparison of the calculated and measured values of slot conductance. The measured values correspond to the value of conductance where the cover is $0.65\lambda_\epsilon$ thick at the average resonant frequency f_R.

Calculation of Resonant Length

Placing a thin dielectric cover over a shunt slot causes a significant change in the resonant length. Figure 8 shows a measured curve of the reduction in resonant length as a function of dielectric constant. One simple method of approximating the resonant length is to assume that the space surrounding the slot is completely filled with a material of dielectric constant ϵ. Then

$$\left(\frac{l}{\lambda_o}\right)_\epsilon = \frac{l/\lambda_o}{\sqrt{\epsilon}} \tag{9}$$

where

$(l/\lambda_o)_\epsilon$ resonant length with a dielectric cover

l/λ_o resonant length with no cover

Figure 12 shows the original measured curve and the one calculated from equation (9). There is obvious disagreement and equation (9) predicts too short a resonant length. This disagreement means that the slot can be considered equivalently filled with a material having a dielectric constant less than ϵ.

As an approach to obtaining an equivalent dielectric constant ϵ_{equiv}, the following approximate analysis was made:

By definition, only the reactive fields are involved in the determination of resonant length. Since the reactive fields are negligible in the far field, only the source fields or fields near the slot are important. An inspection of the previous analyses indicates that far-field theory gives good approximations to conductance problems with covers $0.20\lambda_\epsilon$ thick. Therefore, the reactive fields most probably extend only into very thin layers of dielectric near the slot. The source field may be considered as consisting of time-harmonic charge pairs which result from the excitation voltage V_o across the slot. The displacement current across the slot must terminate in these charge pairs to satisfy continuity conditions. These source charge pairs can then be interchangeably considered as small current elements or Hertz dipoles having a current equal to the displacement current I. This concept is useful since the exact fields of such a source

are known. Near the Hertz dipole or, equivalently, the charge pairs, the field is predominantly electric and is of the so-called quasi-static form. Since only very thin layers appear to be of importance, quasi-static theory can be used to convert the problem to a simple capacitor equivalent as shown in figure 13.

From pages 55 and 56 of reference 8 for electric fields parallel to the interfaces a reduction of the capacitor can be made as shown in figure 14.

The slot then can be considered to be equivalently filled with a material having a dielectric constant ϵ_{equiv} defined as

$$\epsilon_{equiv} = \frac{\epsilon_1 d_1 + \epsilon_2 d_2}{d_1 + d_2} \tag{10}$$

Unfortunately, the distances d_1 and d_2 are unknown. However, by using the Hertz dipole equivalent a relationship between d_1 and d_2 can be obtained. From reference 9 the net radially propagating reactive energy from a Hertz dipole can be given as

$$W = \frac{c}{\epsilon d^3} \tag{11}$$

By assuming an equal distribution of energy on both sides of the slot the following relationship can be obtained:

$$\frac{c}{\epsilon_1 d_1^3} = \frac{c}{\epsilon_2 d_2^3} \tag{12}$$

Therefore

$$d_2^3 = d_1^3 \frac{\epsilon_1}{\epsilon_2} \tag{13}$$

or

$$d_2 = d_1 \sqrt[3]{\frac{\epsilon_1}{\epsilon_2}} \tag{14}$$

Combining equation (10) and equation (14) results in the following equation:

$$\epsilon_{equiv} = \frac{\epsilon_1 d_1 + \epsilon_2 d_2}{d_1 + d_2} = \frac{\epsilon_1 d_1 + \epsilon_2 d_1 \sqrt[3]{\frac{\epsilon_1}{\epsilon_2}}}{d_1 + d_1 \sqrt[3]{\frac{\epsilon_1}{\epsilon_2}}} \tag{15}$$

or

$$\epsilon_{equiv} = \frac{\epsilon_1 + \epsilon_2 \sqrt[3]{\frac{\epsilon_1}{\epsilon_2}}}{1 + \sqrt[3]{\frac{\epsilon_1}{\epsilon_2}}} \tag{16}$$

But

$\epsilon_1 = 1$

$\epsilon_2 = \epsilon$

Therefore, equation (16) becomes

$$\epsilon_{equiv} = \frac{1 + \epsilon^{2/3}}{1 + \epsilon^{-1/3}} \tag{17}$$

A curve of resonant length as a function of dielectric constant can be obtained from

$$\left(\frac{l}{\lambda_o}\right)_\epsilon = \frac{l/\lambda_o}{\sqrt{\epsilon_{equiv}}} \tag{18}$$

where ϵ_{equiv} is given in equation (17). Calculated results obtained by using equation (18) are shown in figure 12.

ARRAYS

Two resonant arrays were designed on the basis of the single-slot conductance measurements, fabricated, and tested. The first design was composed of

25 slots alternately located on opposite sides of the waveguide center line, spaced on $\lambda_g/2$ centers. The second design was similar but was composed of 56 slots. The input VSWR and far-field radiation patterns were measured.

VSWR

The midband VSWR measured less than 1.1 on both the 25-slot and the 56-slot array. The VSWR characteristics of the 25-slot array plotted as a function of frequency for various cover thicknesses are shown in figure 15. The frequency band over which the array can be operated without major degradation of the main lobe shape or amplitude is indicated by the dashed lines in figure 15. Calculations based on single-slot measurements indicate midband variation of VSWR from 1.03 to 1.08 over the range of cover thickness indicated in figure 15. Results similar to those in figure 15 were obtained on the 56-slot array except that the operating band was approximately 0.05 gigacycle.

Radiation Patterns

Since the array designs were the resonant type, the array factor is defined by the discrete-source theory of reference 10 as

$$E(\theta) = \frac{\sin\left(\frac{\beta n d'}{2} \sin\theta\right)}{\frac{\beta n d'}{2} \sin\theta} \tag{19}$$

To a first approximation, the element pattern can be defined by (p. 8-3 of ref. 11)

$$E_1(\theta) = \frac{\cos\left(\frac{\pi}{2} \sin\theta\right)}{\cos\theta} \tag{20}$$

based on the assumption that the slot is located in an infinite ground plane surrounded by free space. The array pattern can be obtained by multiplying equation (19) by equation (20) (pattern multiplication) and assuming negligible coupling between elements.

Calculations of array patterns were made and are compared with measured patterns in figure 16. Agreement between calculated and measured patterns indicates that mutual coupling is negligible for an array of dielectric-covered shunt slots. It should be noted that no unusual care was exercised in fitting the dielectric covers to the surface of the waveguide. It is therefore believed that for large arrays of shunt slots the tolerance on cover fit is not unduly critical. Within the operating band previously indicated in figure 15, the

patterns were similar to those given at midband except for changes in the level and position of lower order sidelobes.

CONCLUDING REMARKS

The primary purpose of this study was to determine the design parameters for dielectric-covered shunt-slot arrays, where the thickness of the cover was changing as a result of reentry environment. Array designs that are relatively insensitive to dielectric-cover properties are available for materials having dielectric constants less than 4 over the normal waveguide bandwidth.

Approximate theoretical formulas have been developed which give predictions of normalized slot conductance as a function of thickness and resonant length as a function of dielectric constant, accurate to at least 10 percent. It should be noted that these formulas were developed from measurements on materials having dielectric constants less than 4. However, if these formulas are used to extend the data to materials having dielectric constants greater than 4, it can be shown that the voltage standing-wave ratio (VSWR) of shunt-slot arrays will exceed acceptable bounds (VSWR > 2) as a function of cover thickness.

Langley Research Center,
National Aeronautics and Space Administration,
Langley Station, Hampton, Va., August 25, 1964.

REFERENCES

1. Kay, Alan F.: Radomes and Absorbers. Antenna Engineering Handbook, Henry Jasik, ed., McGraw-Hill Book Co., Inc., 1961, pp. 32-1 - 32-40.

2. Meyer, W. A.; Scott, W. G.; and Puro, W. O.: A Compact Dual-Purpose Antenna. IRE Natl. Conv. Record, vol. 6, pt. 1 - Antennas and Propagation; Microwave Theory and Techniques, 1958, pp. 200-203.

3. Croswell, William F.; and Higgins, Robert B.: A Study of Dielectric-Covered Shunt Slots in a Waveguide. Proceedings of NASA Conference on Communicating Through Plasmas of Atmospheric Entry and Rocket Exhaust, NASA SP-52, 1964, pp. 115-129.

4. Ginzton, Edward L.: Microwave Measurements. McGraw-Hill Book Co., Inc., 1957, pp. 262-275.

5. Ehrlich, M. J.: Slot-Antenna Arrays. Antenna Engineering Handbook, Henry Jasik, ed., McGraw-Hill Book Co., Inc., 1961, pp. 9-1 - 9-18.

6. Harrington, Roger F.: Time-Harmonic Electromagnetic Fields. McGraw-Hill Book Co., Inc., 1961, p. 138.

7. Eaton, J. E.; Eyges, L. J.; and Macfarlane, G. G.: Linear-Array Antennas and Feeds. Microwave Antenna Theory and Design, Samuel Silver, ed., McGraw-Hill Book Co., Inc., 1949, pp. 257-333.

8. Richmond, Jack H.: Electromagnetic Field and Optic Theory. Techniques for Airborne Radome Design, Thomas E. Tice, ed. WADC Tech. Rep. 57-67, ASTIA Doc. No. AD 142001, U.S. Air Force, Sept. 1957, pp. 23-70.

9. Schelkunoff, Sergei A.; and Friis, Harald T.: Antennas - Theory and Practice. John Wiley & Sons, Inc., 1952, p. 122.

10. Kraus, John D.: Antennas. McGraw-Hill Book Co., Inc., 1950, pp. 57-126 and 356-361.

11. Blass, Judd: Slot Antennas. Antenna Engineering Handbook, Henry Jasik, ed., McGraw-Hill Book Co., Inc., 1961, pp. 8-1 - 8-16.

TABLE I

TEST SAMPLES

Sample	Slot displacement, x, in.	Slot length, l, in.	Resonant frequency, f_R, Gc	Normalized conductance, g_n
1	0.066	0.475	11.4	0.029
2	.096	.449	12.0	.042
3	.093	.475	11.5	.053
4	.094	.506	10.8	.059
5	.133	.449	12.2	.072
6	.136	.475	11.5	.097
7	.132	.506	11.0	.111
8	.185	.449	12.4	.115

TABLE II

INDEX TO EXPERIMENTAL DIELECTRIC-COVERED SHUNT-SLOT DATA

Dielectric constant of covering, ϵ	Loss tangent	Figure	Slot displacement, x, in.	Slot length, l, in.	Cover thickness, t, in.	Frequency range, Gc
2.10	0.0002	4(a)	0.066	0.475	0.095 to 0.935	9.4 to 10.7
		4(b)	.096	.449	0.095 to 0.935	10 to 11.4
		4(c)	.093	.475	0.095 to 0.935	9.2 to 11.0
		4(d)	.094	.506	0.095 to 0.935	9.0 to 10.5
		4(e)	.133	.449	0.095 to 0.935	10 to 11.6
		4(f)	.136	.475	0.095 to 0.935	9.0 to 10.8
		4(g)	.132	.506	0.095 to 0.935	9.0 to 10.4
		4(h)	.185	.449	0.095 to 0.935	10.1 to 11.4
2.78	0.020	5(a)	0.066	0.475	0.090 to 0.710	8.9 to 10.2
		5(b)	.096	.449	0.090 to 0.710	9.2 to 11.0
		5(c)	.093	.475	0.090 to 0.710	8.6 to 10.4
		5(d)	.094	.506	0.090 to 0.710	8.2 to 9.8
		5(e)	.133	.449	0.120 to 0.860	8.7 to 11.0
		5(f)	.136	.475	0.090 to 0.710	8.7 to 10.3
		5(g)	.132	.506	0.120 to 0.800	8.2 to 10.0
		5(h)	.185	.449	0.120 to 0.860	8.9 to 11.0
3.31	0.024	6(a)	0.066	0.475	0.100 to 0.900	8.5 to 10.0
		6(b)	.096	.449	0.100 to 0.900	8.7 to 10.1
		6(c)	.093	.475	0.100 to 0.900	8.6 to 9.8
		6(d)	.094	.506	0.100 to 0.900	8.0 to 9.2
		6(e)	.133	.449	0.100 to 0.900	8.0 to 10.1
		6(f)	.136	.475	0.100 to 0.900	8.2 to 9.6
		6(g)	.132	.506	0.100 to 0.900	7.7 to 9.2
		6(h)	.185	.449	0.100 to 0.900	8.9 to 10.2
3.78	0.0001	7(a)	0.066	0.475	0.125 to 0.875	8.0 to 9.2
		7(b)	.096	.449	0.125 to 0.875	8.4 to 9.6
		7(c)	.093	.475	0.125 to 0.875	8.0 to 9.2
		7(d)	.094	.506	0.125 to 0.875	7.6 to 8.7
		7(e)	.133	.449	0.125 to 0.875	8.4 to 9.6
		7(f)	.136	.475	0.125 to 0.875	8.0 to 9.2
		7(g)	.132	.506	0.125 to 0.875	7.7 to 8.6
		7(h)	.185	.449	0.125 to 0.875	8.4 to 9.6

TABLE III

COMPARISON OF MEASURED AND CALCULATED NORMALIZED CONDUCTANCE

Sample	Normalized conductance for cover having -							
	ϵ = 2.10		ϵ = 2.78		ϵ = 3.31		ϵ = 3.78	
	Calculated	Measured	Calculated	Measured	Calculated	Measured	Calculated	Measured
1	0.019	0.021	0.019	0.019	0.019	0.020	0.024	0.021
2	.028	.028	.028	.026	.029	.025	.031	.029
3	.037	.036	.036	.030	.037	.034	.042	.038
4	.049	.046	.048	.045	.051	.047	.053	.050
5	.050	.044	.048	.042	.048	.042	.053	.048
6	.071	.066	.062	.056	.061	.057	.063	.069
7	.080	.081	.075	.077	.075	.078	.071	.090
8	.079	.077	.072	.075	.070	.066	.068	.083

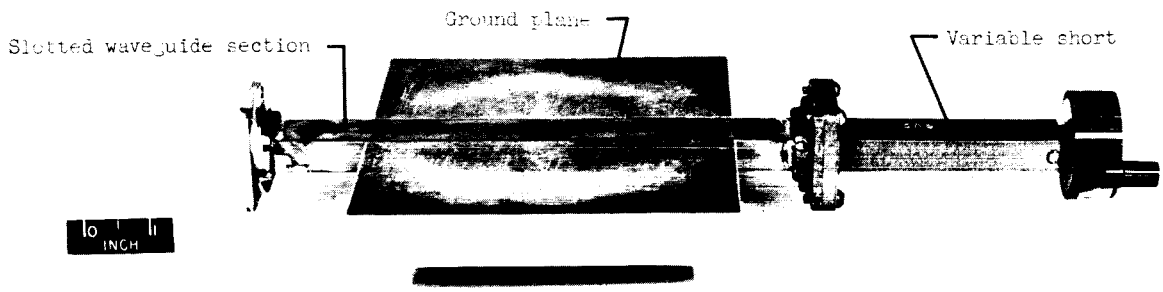

Figure 1.- Test sample. L-63-8917

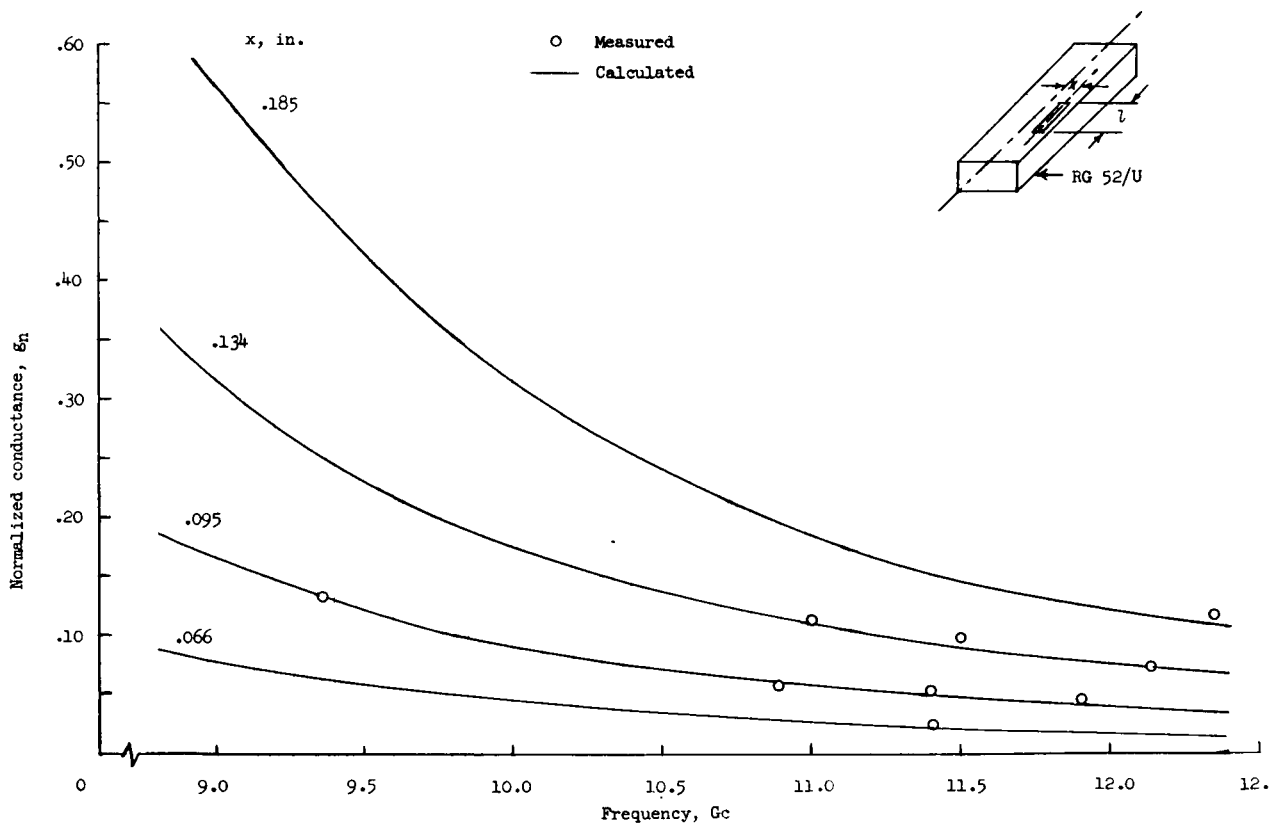

Figure 2.- Normalized resonant conductance as a function of resonant frequency for various slot displacements.

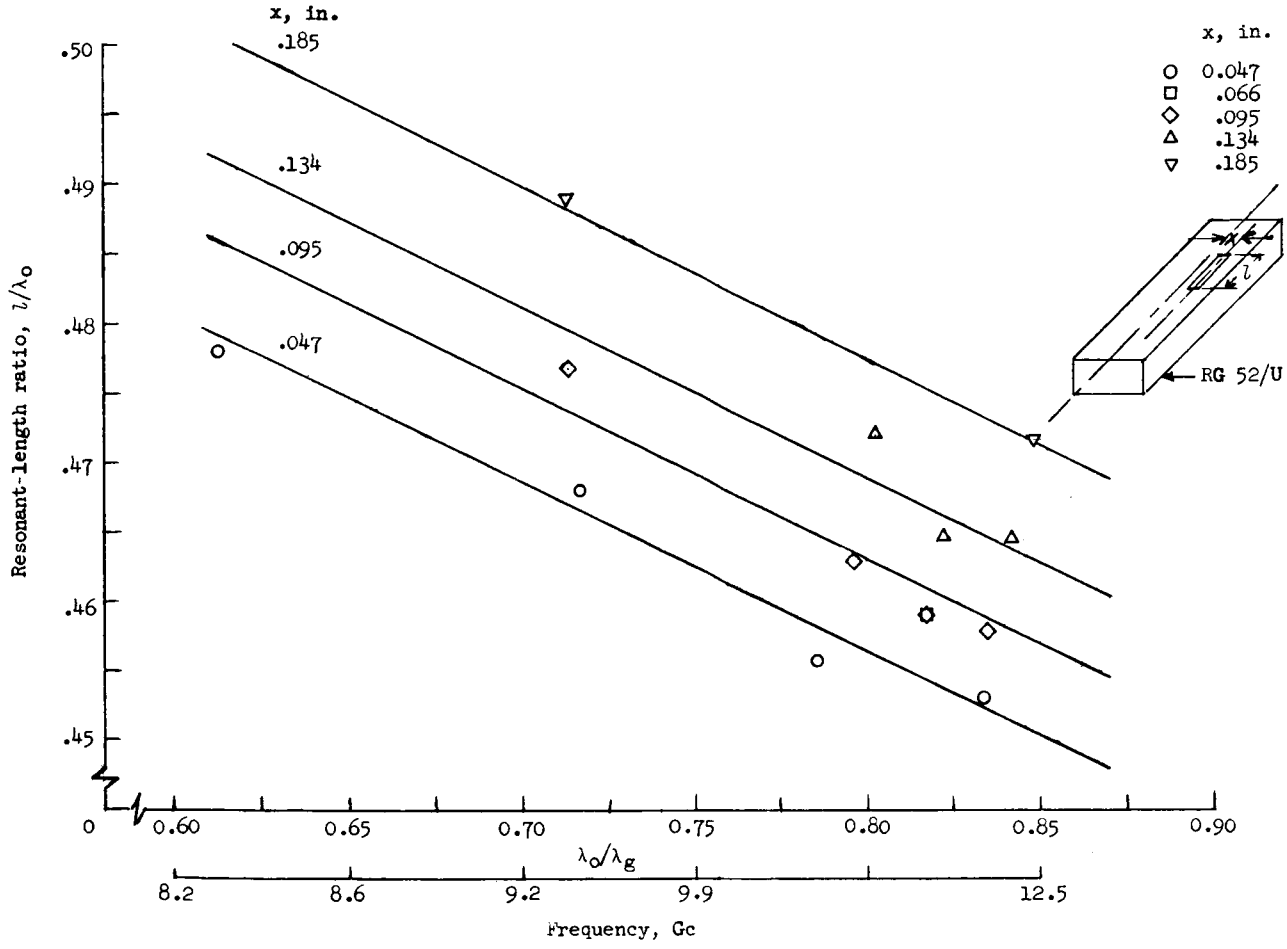

Figure 3.- Resonant length as a function of ratio of free-space wavelength to waveguide wavelength for various slot displacements.

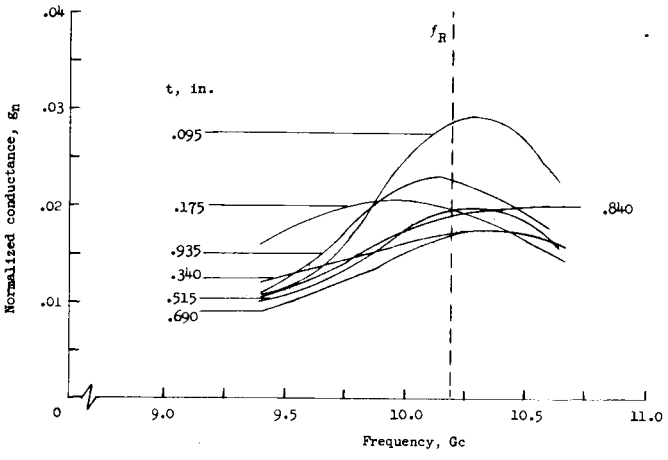

(a) x = 0.066 inch; l = 0.475 inch; f_o = 11.4 gigacycles.

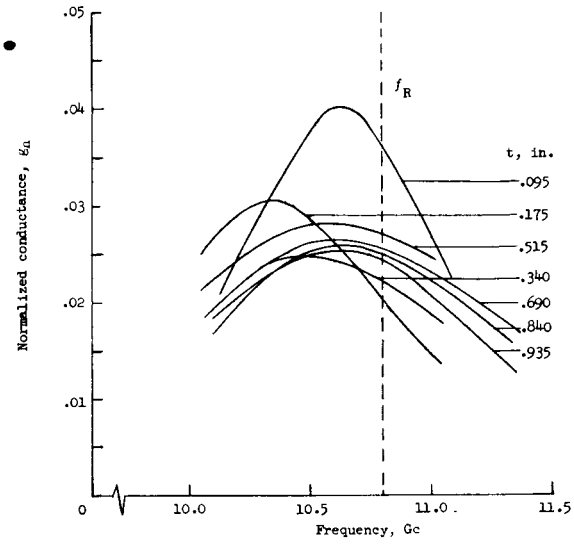

(b) x = 0.096 inch; l = 0.449 inch; f_o = 12.0 gigacycles.

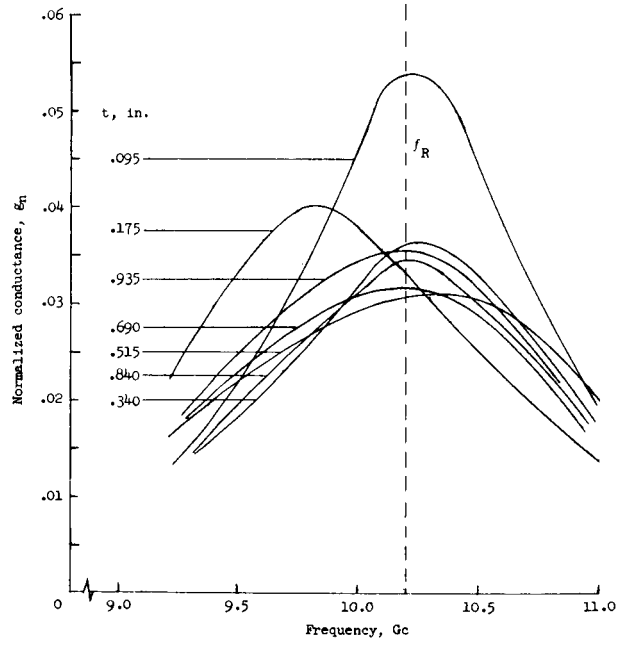

(c) x = 0.093 inch; l = 0.475 inch; f_o = 11.5 gigacycles.

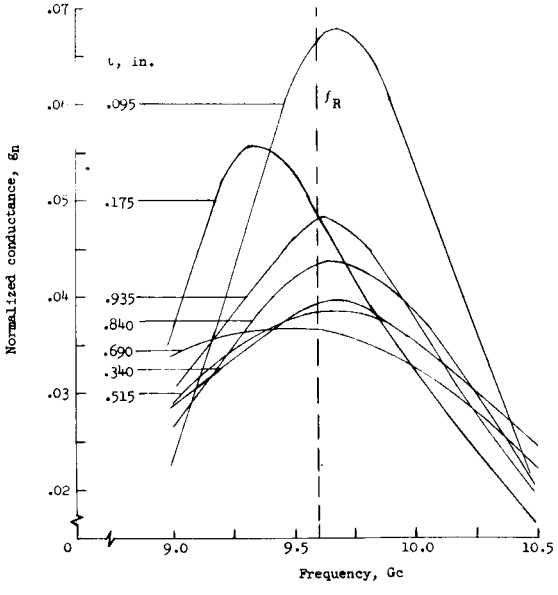

(d) x = 0.094 inch; l = 0.506 inch; f_o = 10.8 gigacycles.

Figure 4.- Normalized conductance as a function of frequency for various cover thicknesses. ϵ = 2.10.

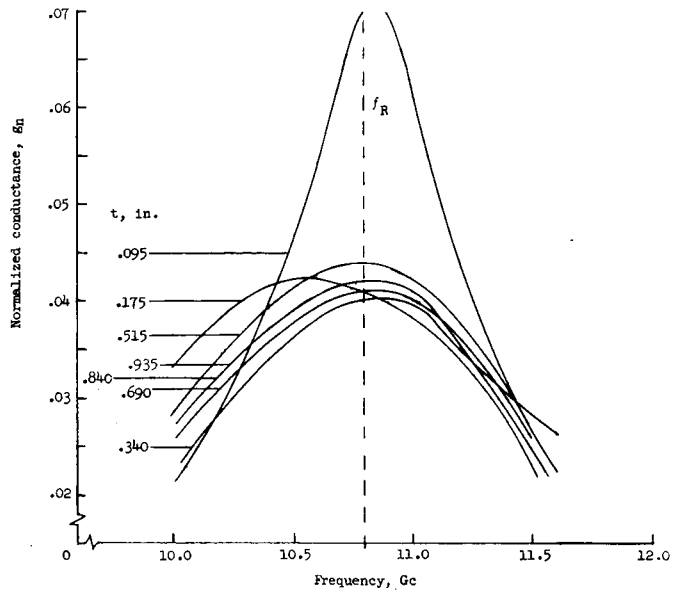

(e) x = 0.133 inch; l = 0.449 inch; f_o = 12.2 gigacycles.

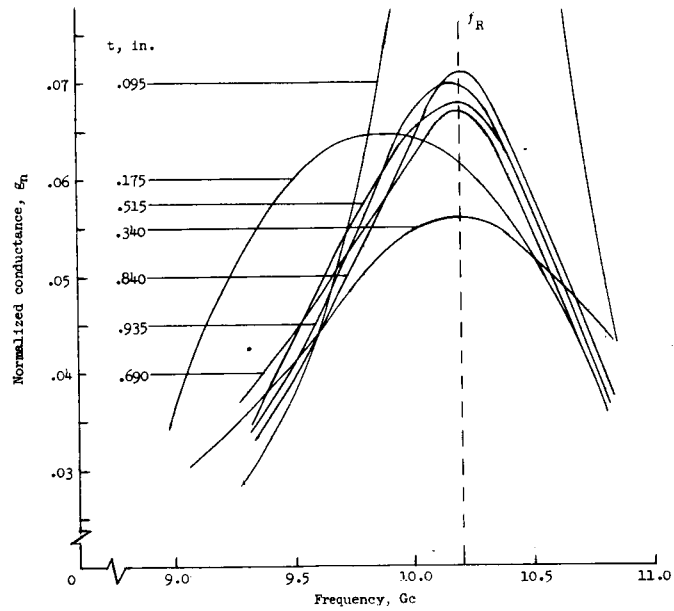

(f) x = 0.136 inch; l = 0.475 inch; f_o = 11.5 gigacycles.

Figure 4.- Continued.

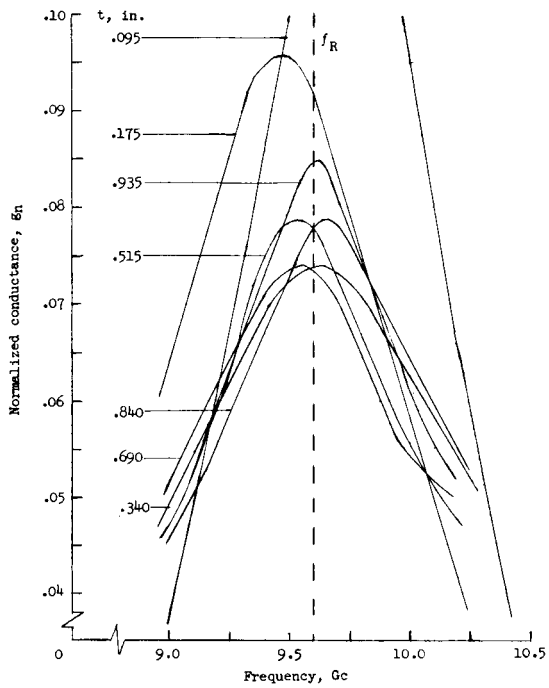

(g) x = 0.132 inch; l = 0.506 inch; f_o = 11.0 gigacycles.

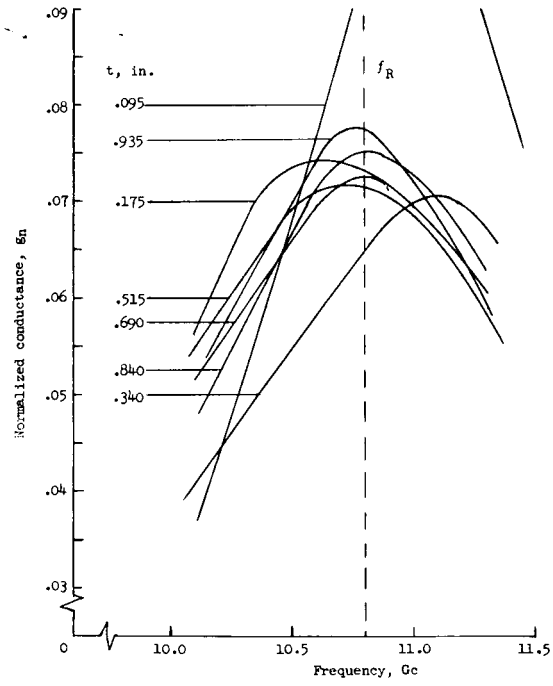

(h) x = 0.185 inch; l = 0.449 inch; f_o = 12.4 gigacycles.

Figure 4.- Concluded.

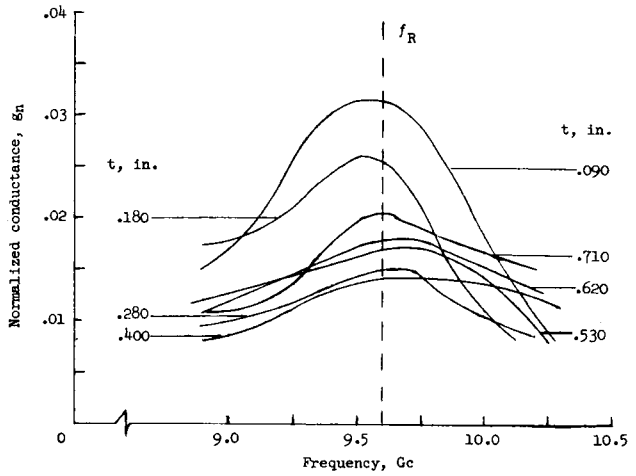

(a) x = 0.066 inch; l = 0.475 inch; f_o = 11.4 gigacycles.

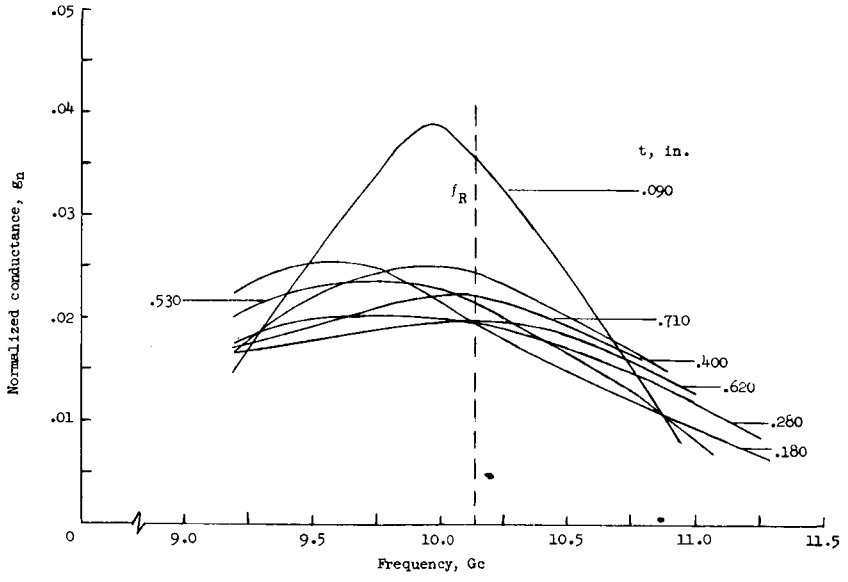

(b) x = 0.096 inch; l = 0.449 inch; f_o = 12.0 gigacycles.

Figure 5.- Normalized conductance as a function of frequency for various cover thicknesses. ϵ = 2.78.

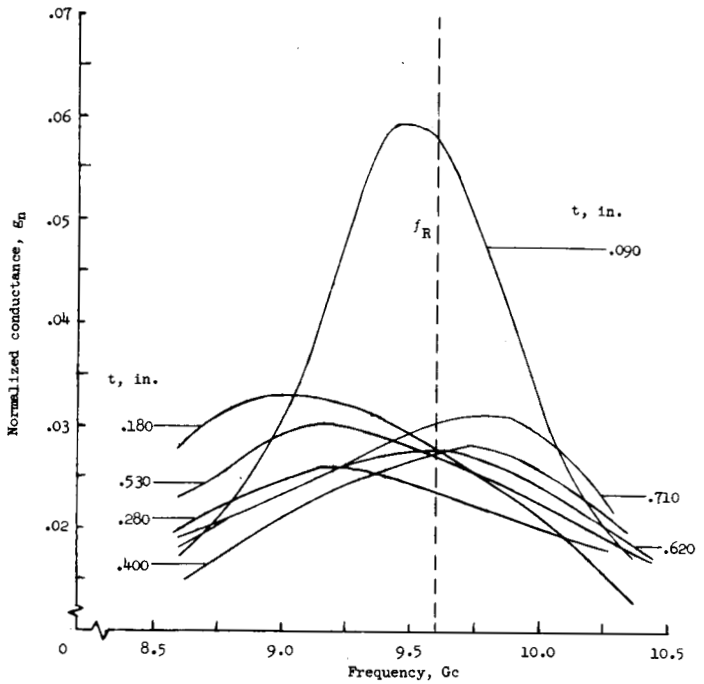

(c) x = 0.093 inch; l = 0.475 inch; f_o = 11.5 gigacycles.

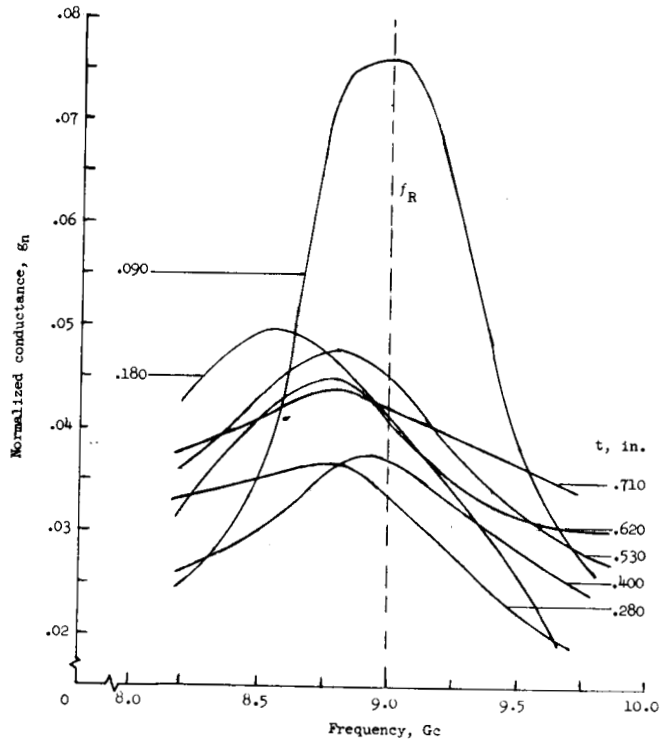

(d) x = 0.094 inch; l = 0.506 inch; f_o = 10.8 gigacycles.

Figure 5.- Continued.

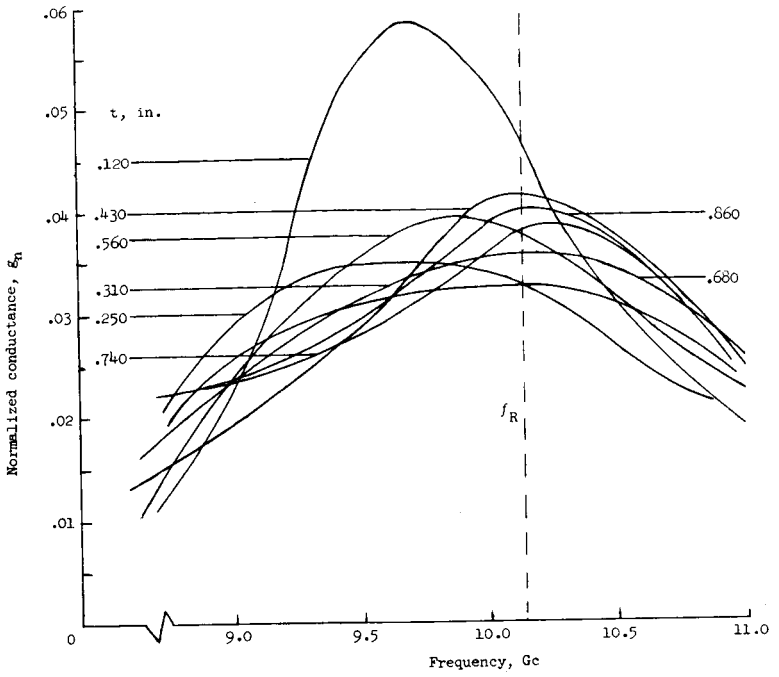

(e) x = 0.133 inch; l = 0.449 inch; f_o = 12.2 gigacycles.

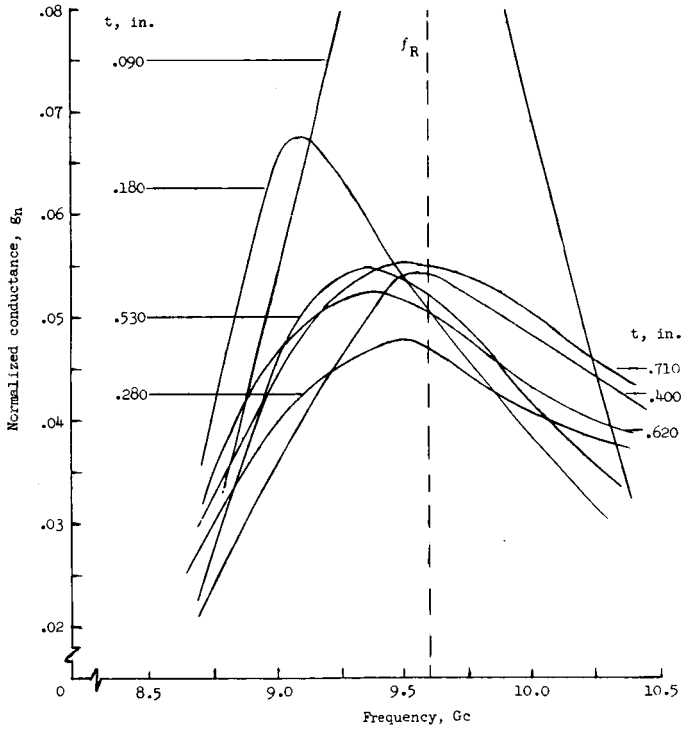

(f) x = 0.136 inch; l = 0.475 inch; f_o = 11.5 gigacycles.

Figure 5.- Continued.

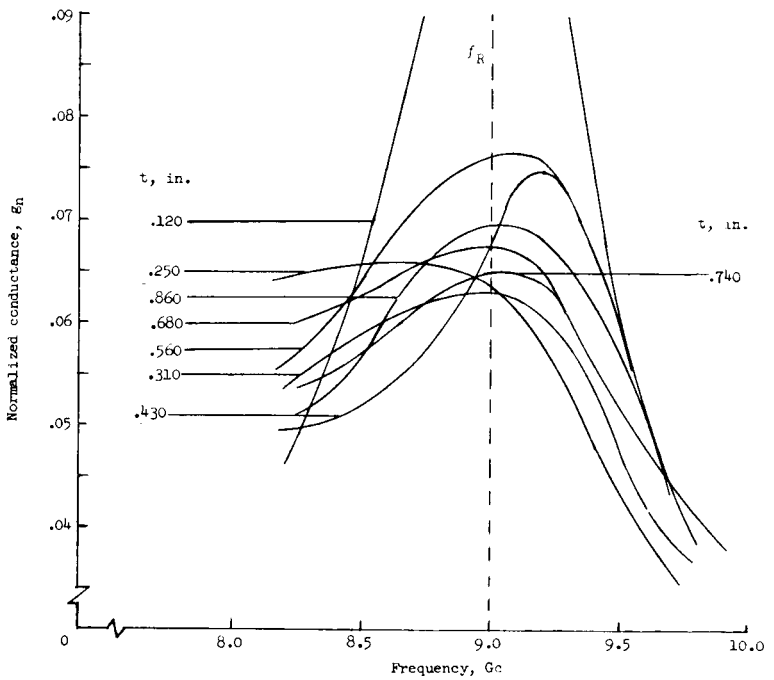

(g) x = 0.132 inch; l = 0.506 inch; f_o = 11.0 gigacycles.

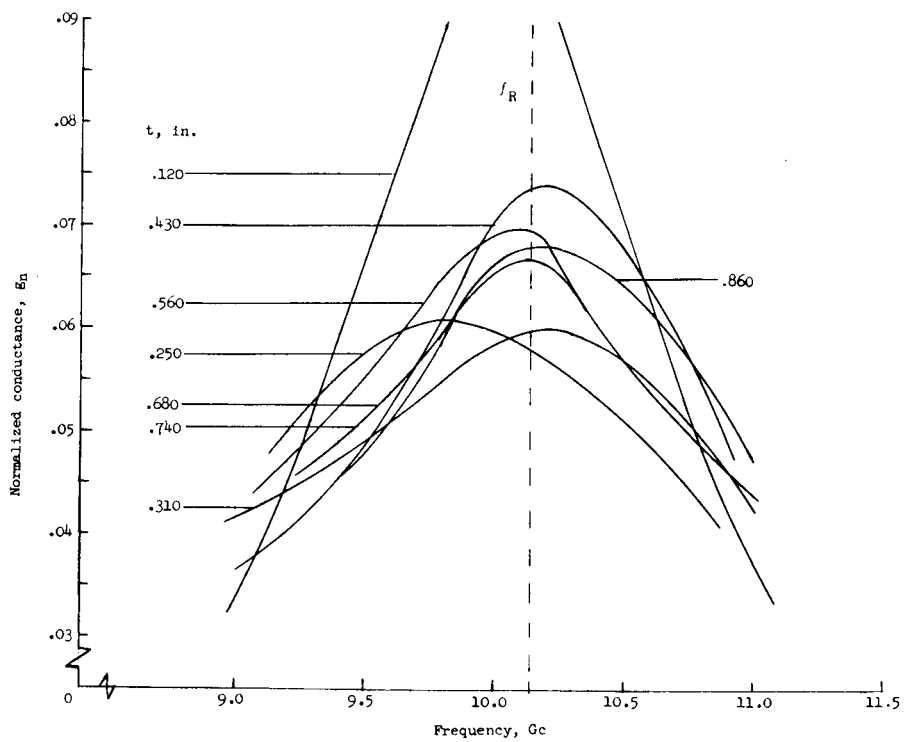

(h) x = 0.185 inch; l = 0.449 inch; f_o = 12.4 gigacycles.

Figure 5.- Concluded.

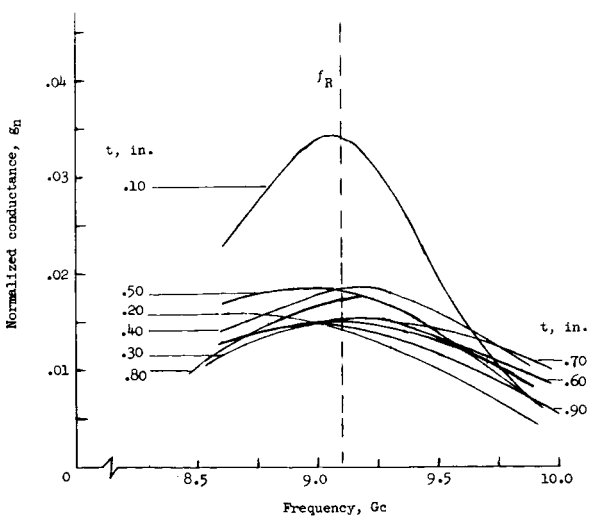

(a) x = 0.066 inch; l = 0.475 inch; f_o = 11.4 gigacycles.

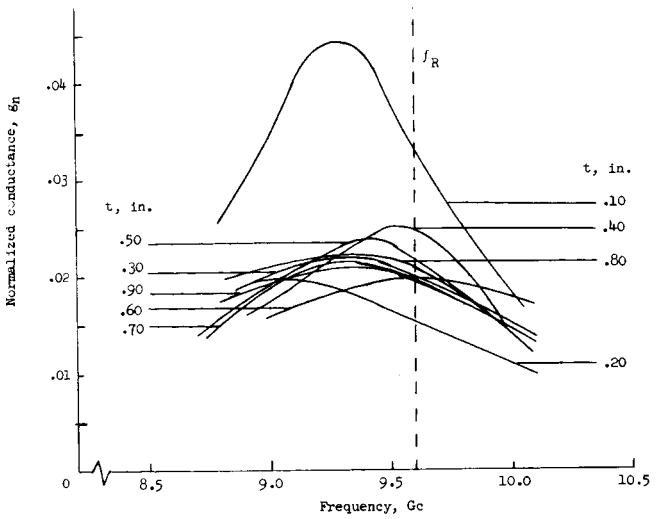

(b) x = 0.096 inch; l = 0.449 inch; f_o = 12.0 gigacycles.

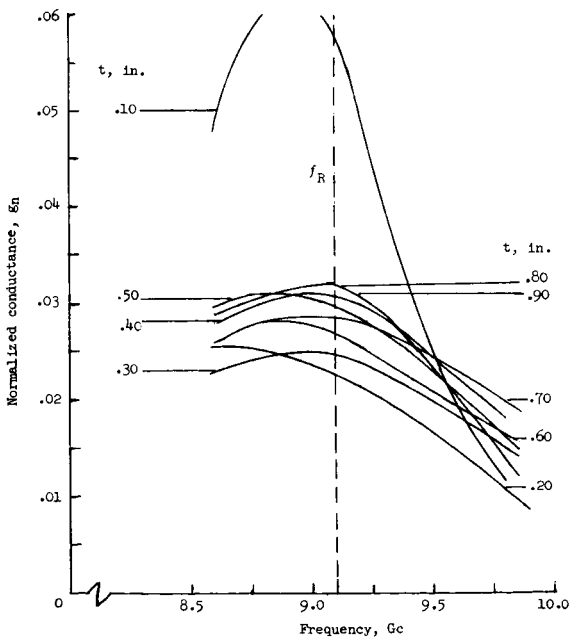

(c) x = 0.093 inch; l = 0.475 inch; f_o = 11.5 gigacycles.

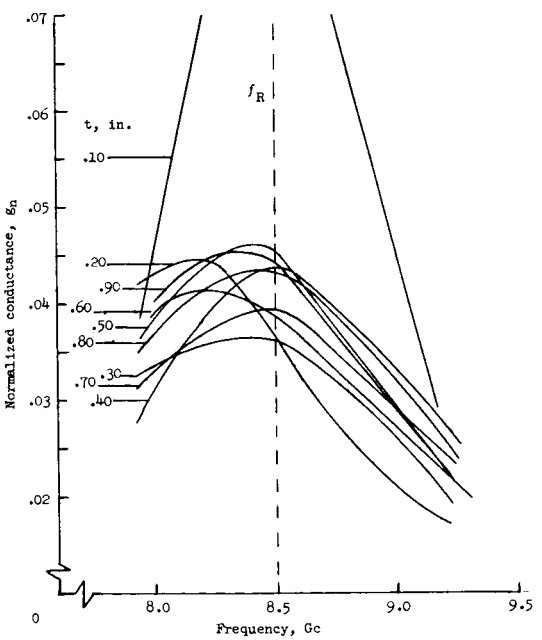

(d) x = 0.094 inch; l = 0.506 inch; f_o = 10.8 gigacycles.

Figure 6.- Normalized conductance as a function of frequency for various cover thicknesses. ϵ = 3.31.

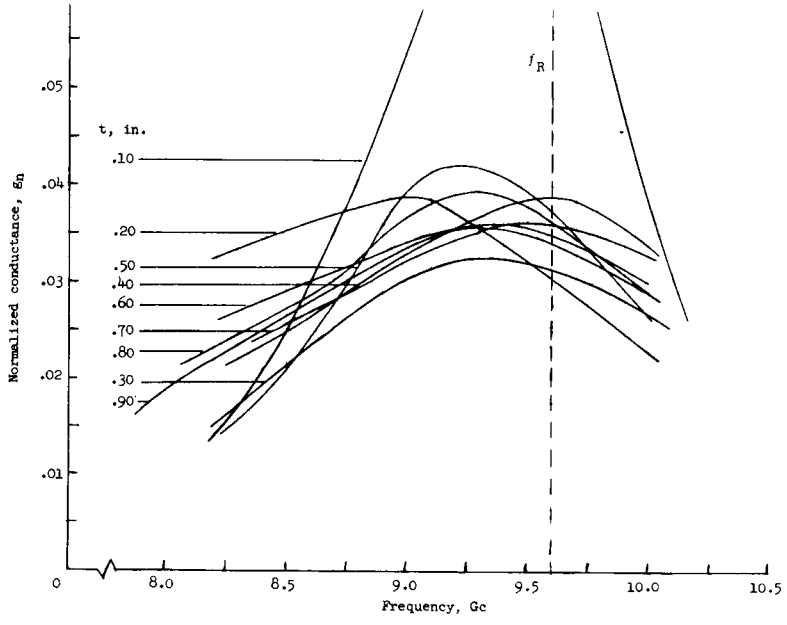

(e) x = 0.133 inch; l = 0.449 inch; f_o = 12.2 gigacycles.

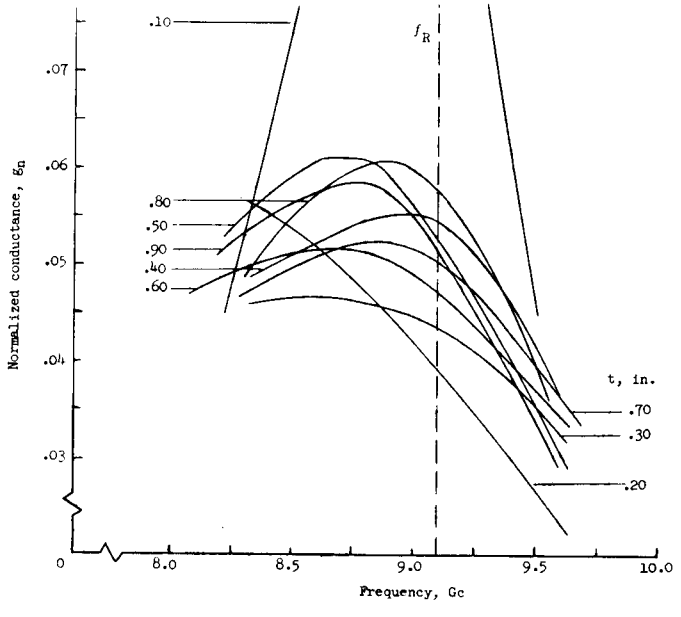

(f) x = 0.136 inch; l = 0.475 inch; f_o = 11.5 gigacycles.

Figure 6.- Continued.

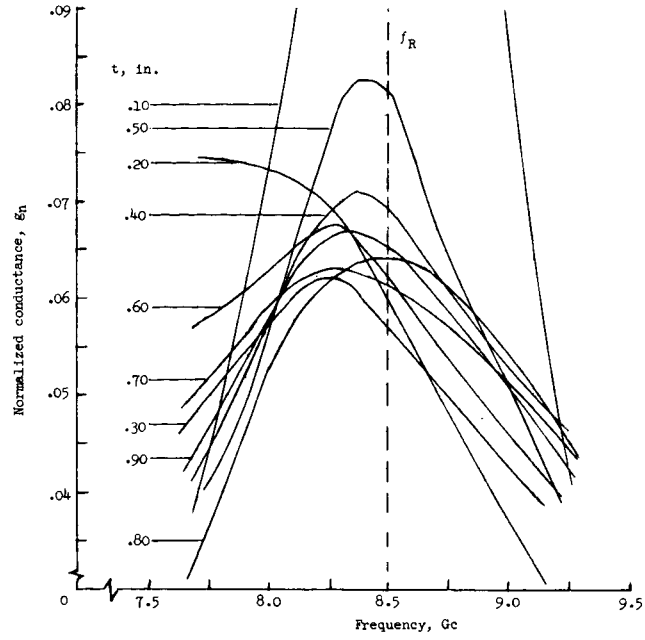

(g) x = 0.132 inch; l = 0.506 inch; f_o = 11.0 gigacycles.

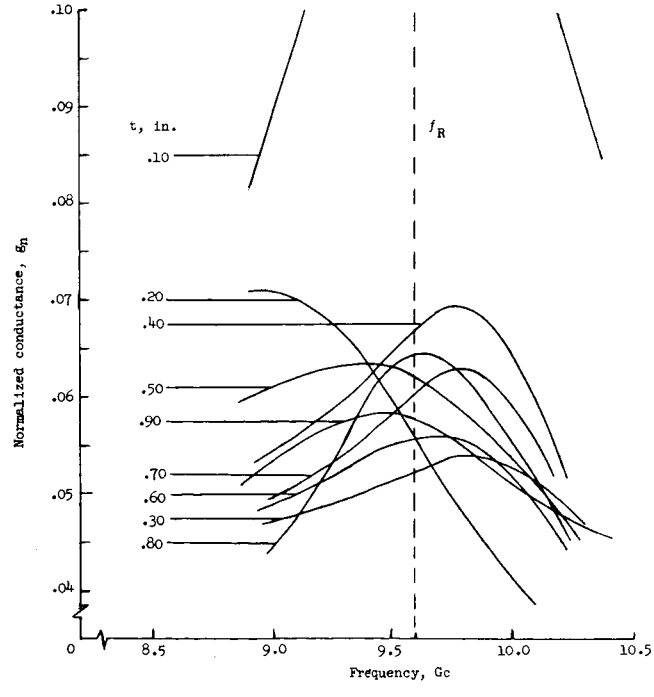

(h) x = 0.185 inch; l = 0.449 inch; f_o = 12.4 gigacycles.

Figure 6.- Concluded.

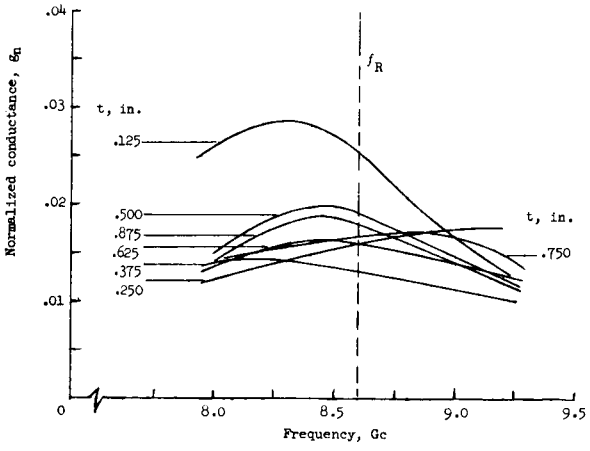

(a) x = 0.066 inch; l = 0.475 inch; f_o = 11.4 gigacycles.

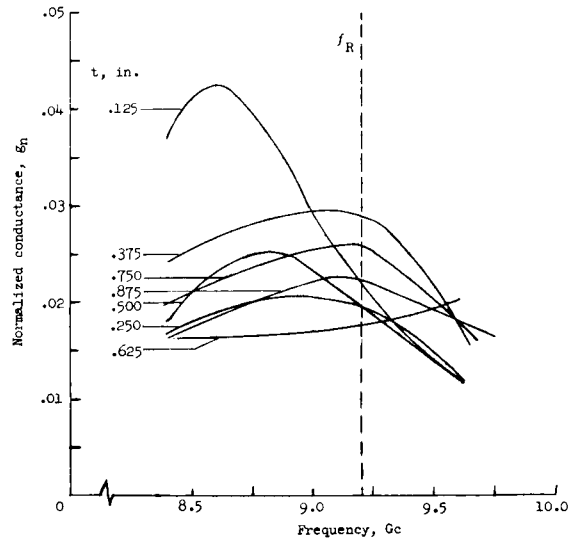

(b) x = 0.096 inch; l = 0.449 inch; f_o = 12.0 gigacycles.

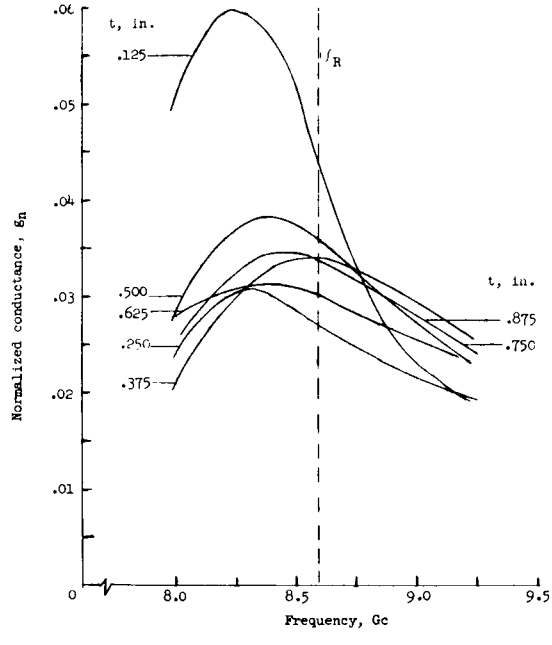

(c) x = 0.093 inch; l = 0.475 inch; f_o = 11.5 gigacycles.

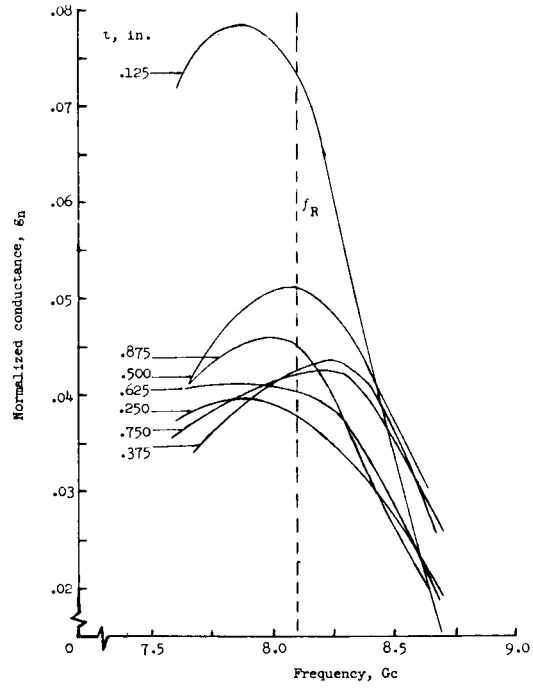

(d) x = 0.094 inch; l = 0.506 inch; f_o = 10.8 gigacycles.

Figure 7.- Normalized conductance as a function of frequency for various cover thicknesses. ϵ = 3.78.

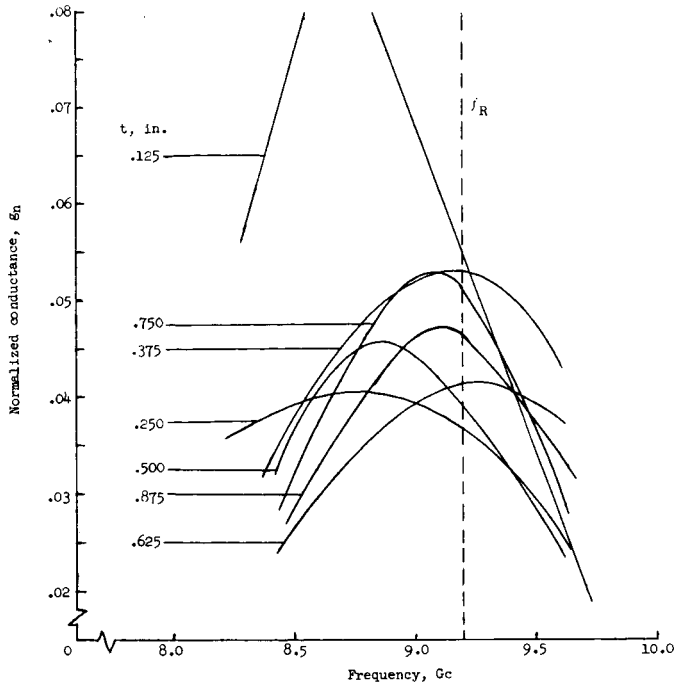

(e) x = 0.133 inch; l = 0.449 inch; f_o = 12.2 gigacycles.

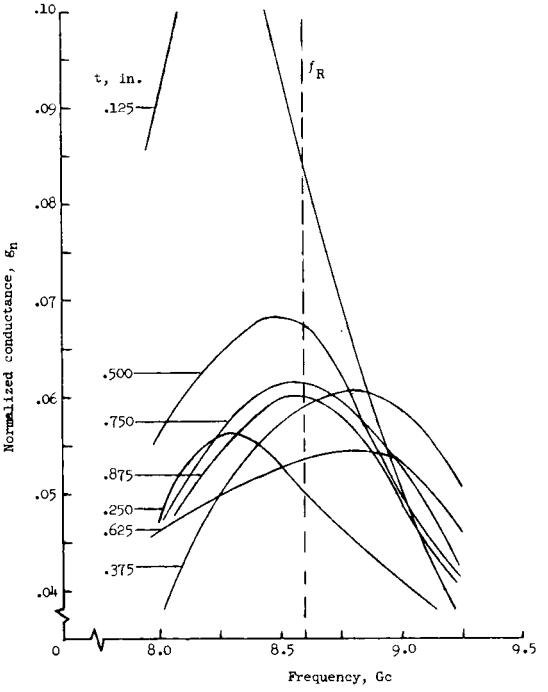

(f) x = 0.136 inch; l = 0.475 inch; f_o = 11.5 gigacycles.

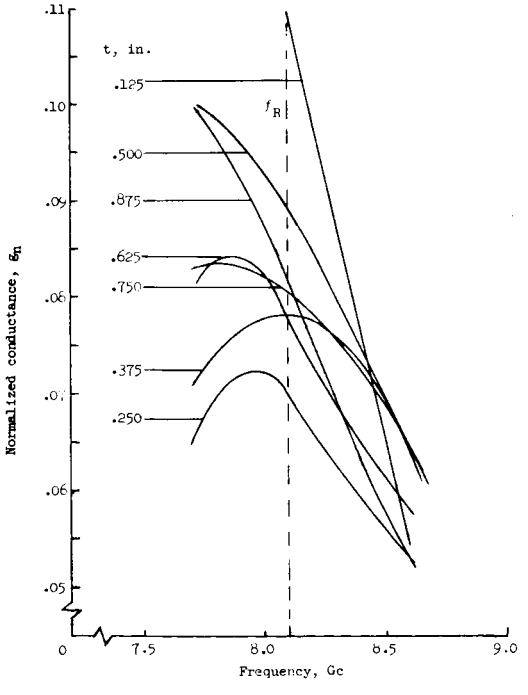

(g) x = 0.132 inch; l = 0.506 inch; f_o = 11.0 gigacycles.

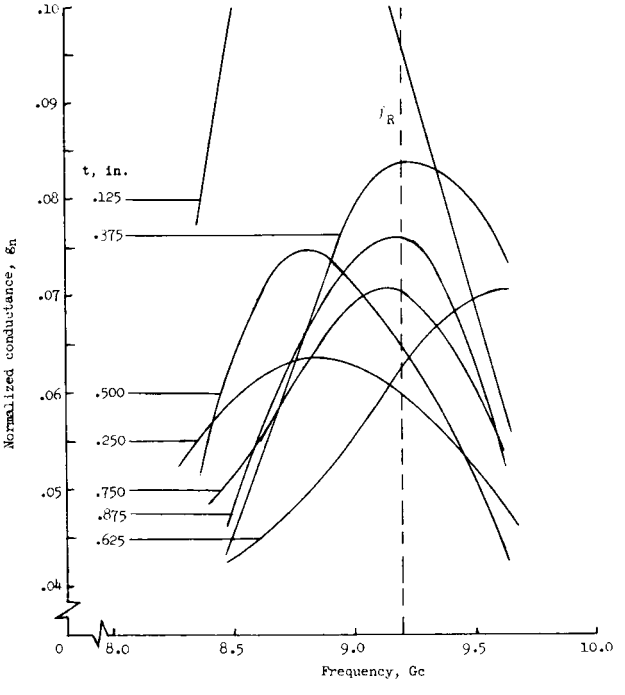

(h) x = 0.185 inch; l = 0.449 inch; f_o = 12.4 gigacycles.

Figure 7.- Concluded.

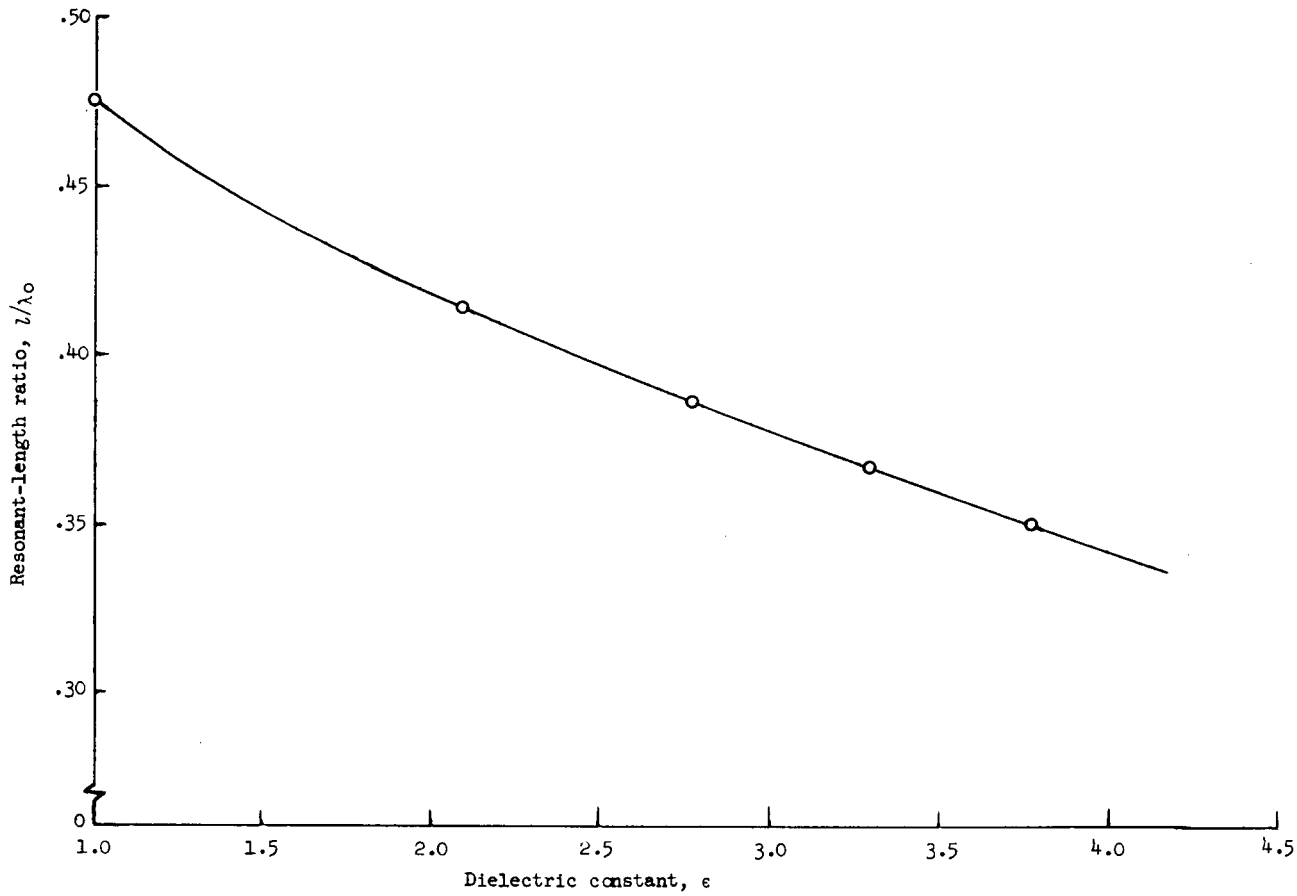

Figure 8.- Resonant-length ratio as a function of dielectric constant.

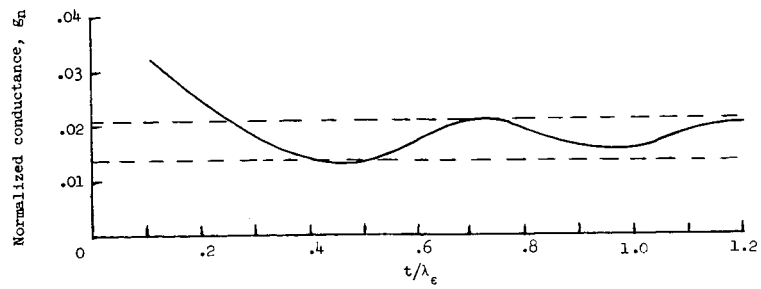

(a) $\epsilon = 3.78$; $f_R = 8.6$ gigacycles.

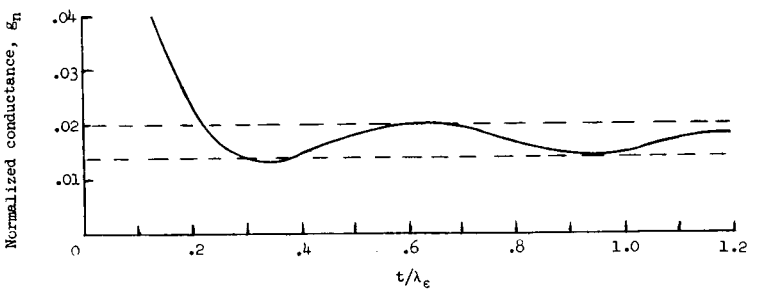

(b) $\epsilon = 3.31$; $f_R = 9.1$ gigacycles.

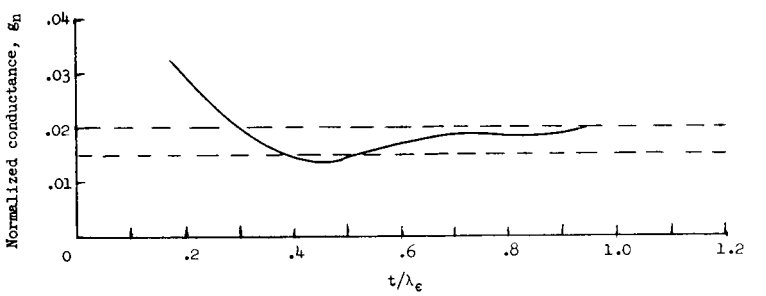

(c) $\epsilon = 2.78$; $f_R = 9.6$ gigacycles.

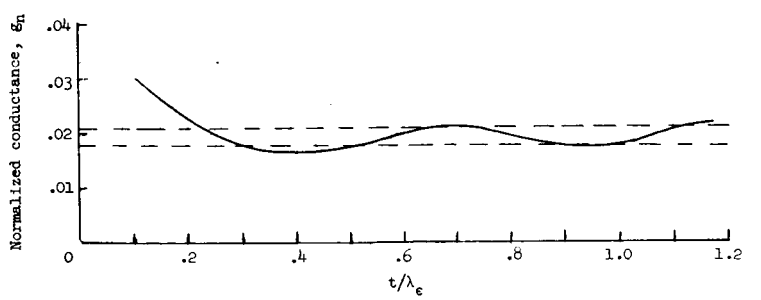

(d) $\epsilon = 2.10$; $f_R = 10.2$ gigacycles.

Figure 9.- Normalized conductance as a function of cover thickness in terms of wavelength in the dielectric for $x = 0.066$ inch and $l = 0.475$ inch.

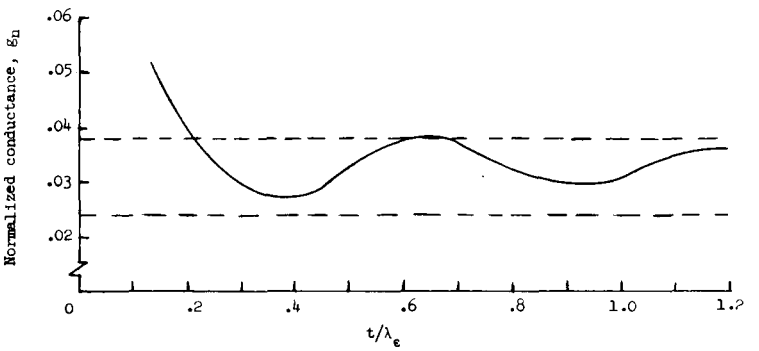

(a) $\epsilon = 3.78$; $f_R = 8.6$ gigacycles.

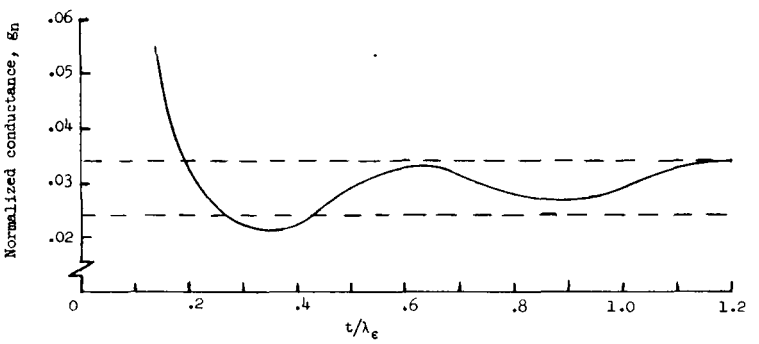

(b) $\epsilon = 3.31$; $f_R = 9.1$ gigacycles.

Figure 10.- Normalized conductance as a function of cover thickness in terms of wavelength in the dielectric for $x = 0.093$ inch and $l = 0.475$ inch.

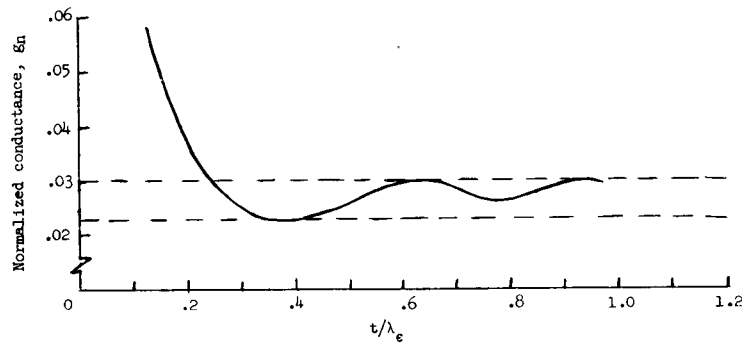

(c) $\epsilon = 2.78$; $f_R = 9.6$ gigacycles.

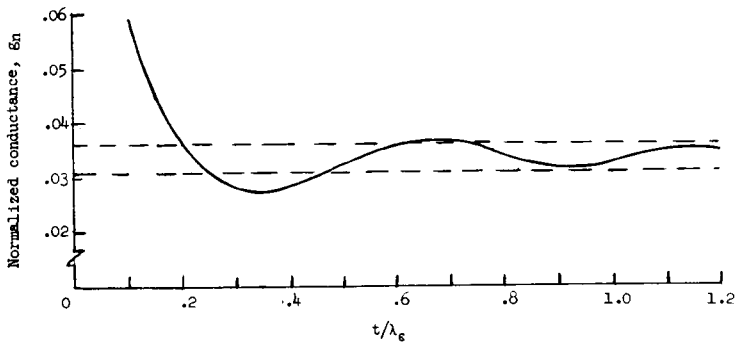

(d) $\epsilon = 2.10$; $f_R = 10.2$ gigacycles.

Figure 10.- Concluded.

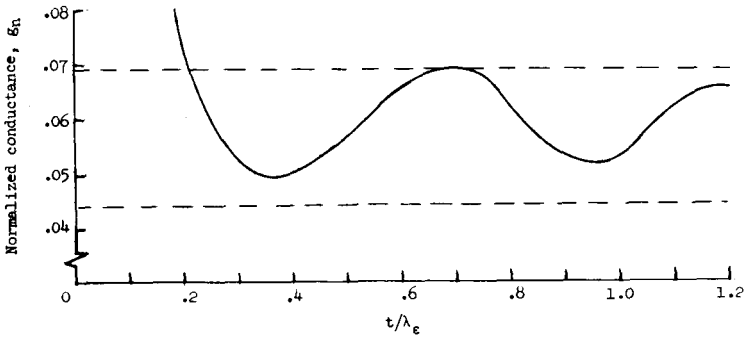

(a) $\epsilon = 3.78$; $f_R = 8.6$ gigacycles.

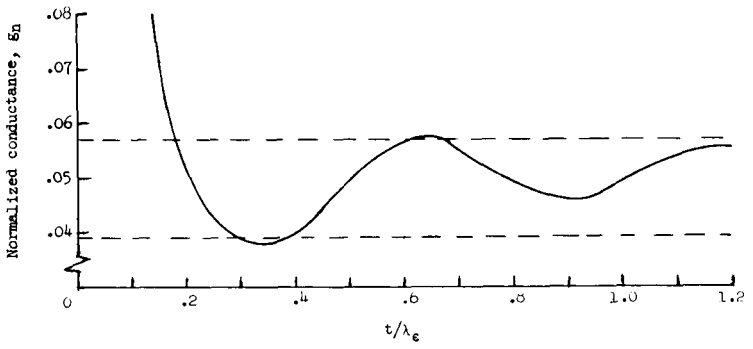

(b) $\epsilon = 3.31$; $f_R = 9.1$ gigacycles.

Figure 11.- Normalized conductance as a function of cover thickness in terms of wavelength in the dielectric for $x = 0.136$ inch and $l = 0.475$ inch.

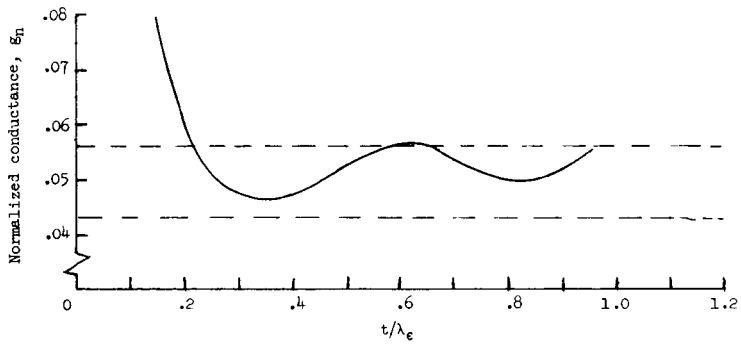

(c) $\epsilon = 2.78$; $f_R = 9.6$ gigacycles.

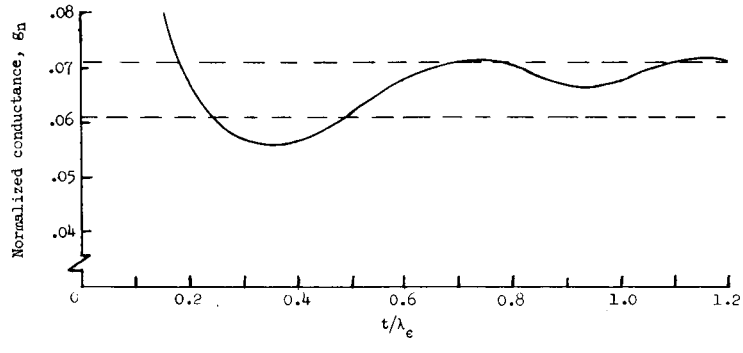

(d) $\epsilon = 2.10$; $f_R = 10.2$ gigacycles.

Figure 11.- Concluded.

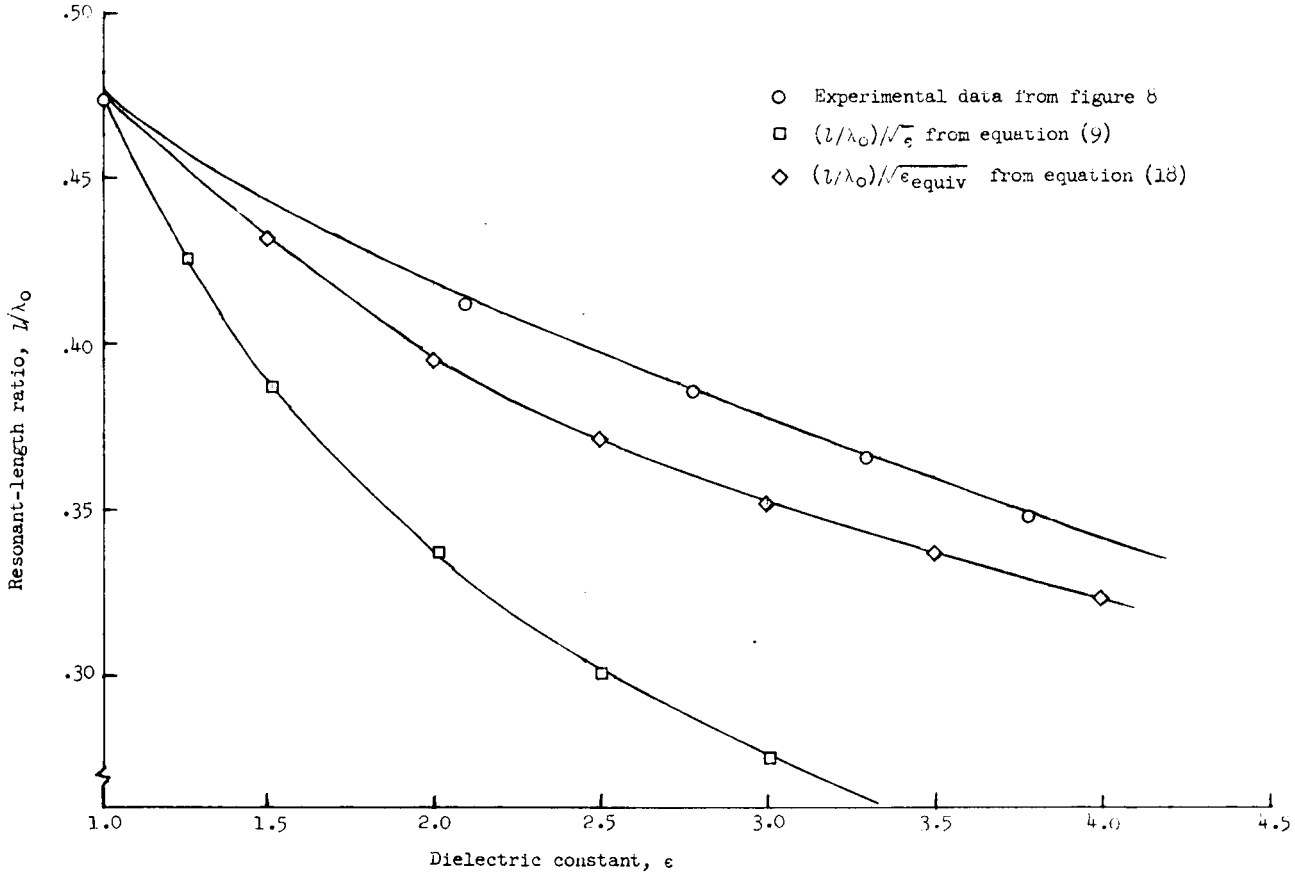

Figure 12.- Comparison of theoretical and experimental values of resonant length as a function of dielectric constant.

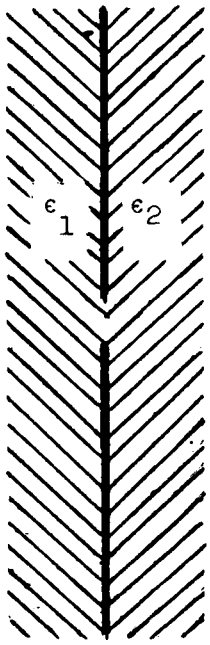

(a) Slot in ground plane.

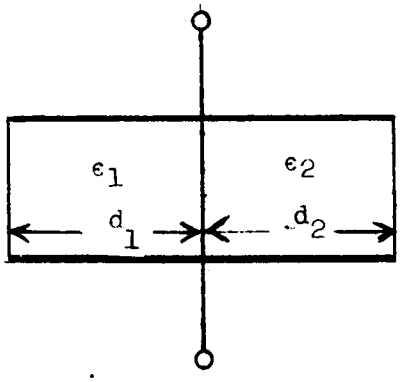

(b) Equivalent capacitor.

Figure 13.- Reduction of slot in ground plane to a quasi-static equivalent.

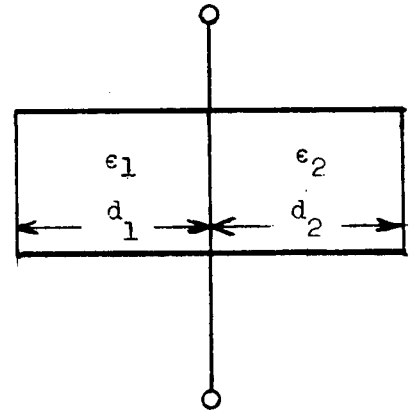

(a) Original form.

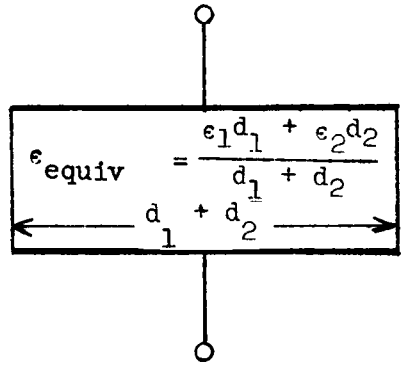

(b) Equivalent form.

Figure 14.- Reduction of quasi-static forms.

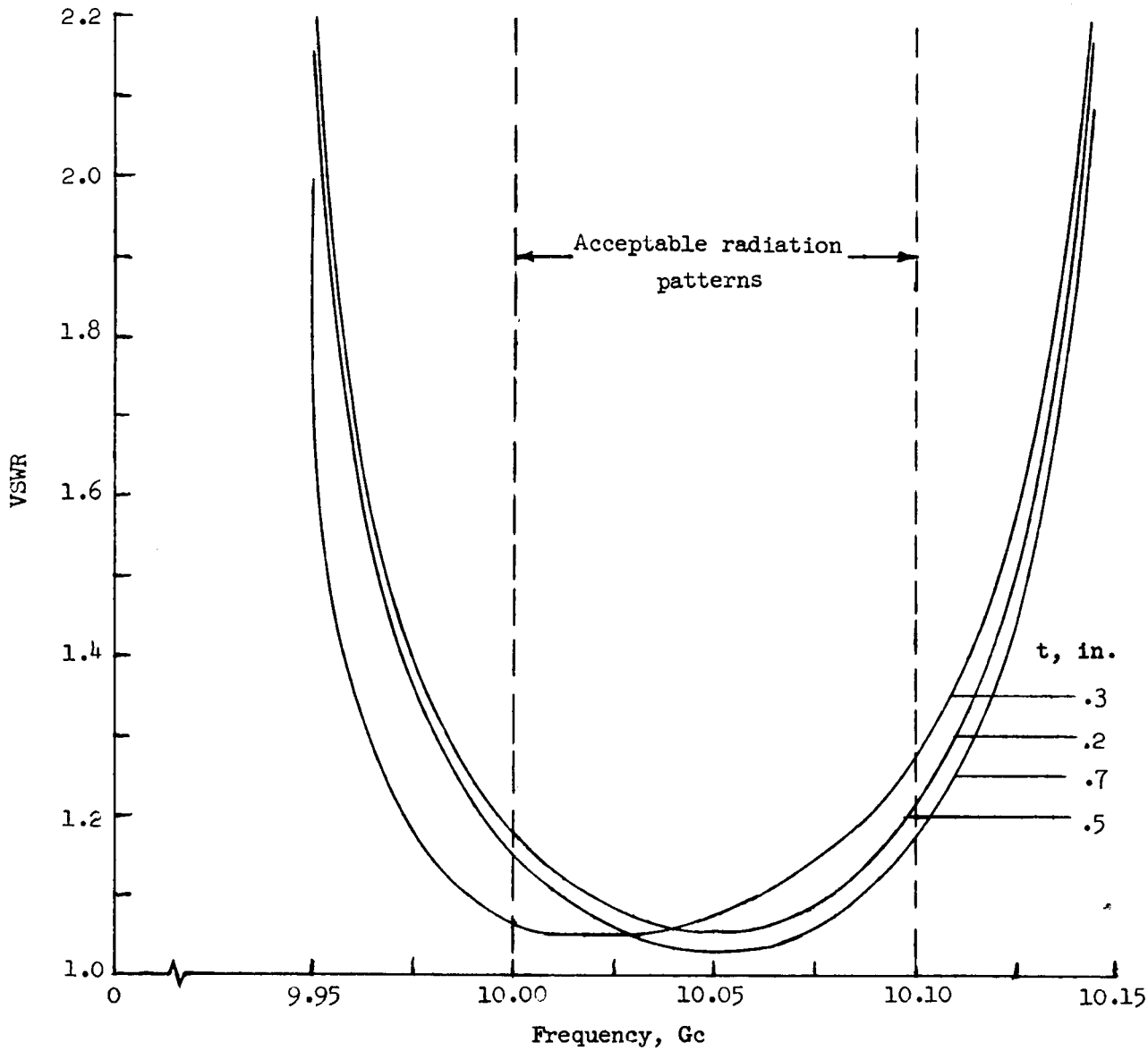

Figure 15.- VSWR of 25-slot array as a function of frequency for various cover thicknesses. $\epsilon = 2.78$.

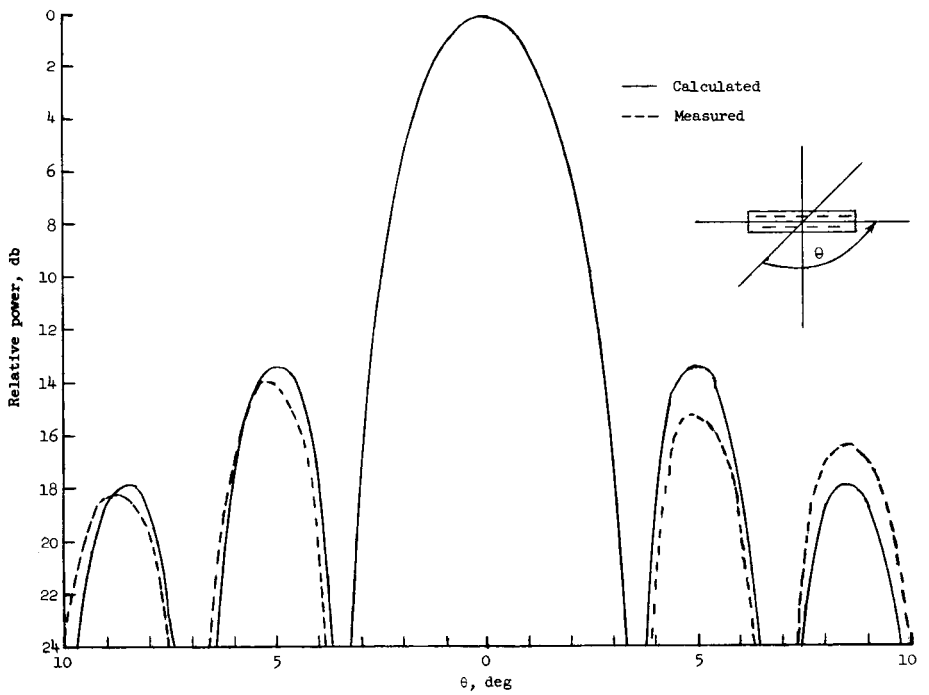

(a) 25-slot array; f = 10.05 gigacycles.

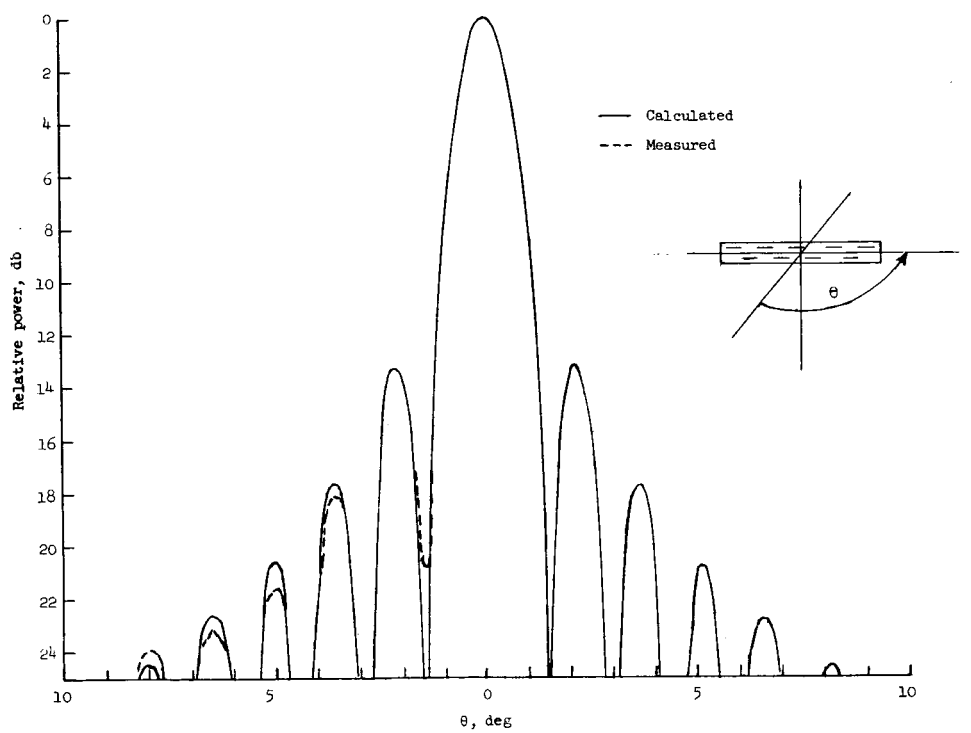

(b) 56-slot array; f = 9.41 gigacycles.

Figure 16.- Principal H-plane radiation patterns of linear resonant arrays.

"The aeronautical and space activities of the United States shall be conducted so as to contribute . . . to the expansion of human knowledge of phenomena in the atmosphere and space. The Administration shall provide for the widest practicable and appropriate dissemination of information concerning its activities and the results thereof."

—NATIONAL AERONAUTICS AND SPACE ACT OF 1958

NASA SCIENTIFIC AND TECHNICAL PUBLICATIONS

TECHNICAL REPORTS: Scientific and technical information considered important, complete, and a lasting contribution to existing knowledge.

TECHNICAL NOTES: Information less broad in scope but nevertheless of importance as a contribution to existing knowledge.

TECHNICAL MEMORANDUMS: Information receiving limited distribution because of preliminary data, security classification, or other reasons.

CONTRACTOR REPORTS: Technical information generated in connection with a NASA contract or grant and released under NASA auspices.

TECHNICAL TRANSLATIONS: Information published in a foreign language considered to merit NASA distribution in English.

TECHNICAL REPRINTS: Information derived from NASA activities and initially published in the form of journal articles.

SPECIAL PUBLICATIONS: Information derived from or of value to NASA activities but not necessarily reporting the results of individual NASA-programmed scientific efforts. Publications include conference proceedings, monographs, data compilations, handbooks, sourcebooks, and special bibliographies.

Details on the availability of these publications may be obtained from:

SCIENTIFIC AND TECHNICAL INFORMATION DIVISION

NATIONAL AERONAUTICS AND SPACE ADMINISTRATION

Washington, D.C. 20546